PSU-IRL-SCI-402

Classification Numbers 1.9.3 and 1.9.4

THE PENNSYLVANIA STATE UNIVERSITY

IONOSPHERIC RESEARCH

Scientific Report 402

NEUTRAL ATMOSPHERIC MODELS COMPATIBLE WITH SATELLITE ORBITAL DECAY AND INCOHERENT SCATTER MEASUREMENTS
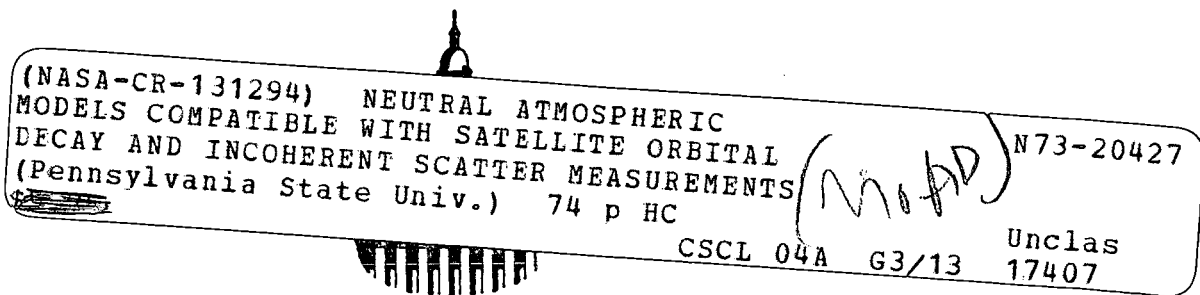
by

James Lee Rohrbaugh

November 7, 1972

IONOSPHERE RESEARCH LABORATORY

(NASA-CR-131294) NEUTRAL ATMOSPHERIC MODELS COMPATIBLE WITH SATELLITE ORBITAL DECAY AND INCOHERENT SCATTER MEASUREMENTS (Pennsylvania State Univ.) 74 p HC

N73-20427

CSCL 04A   G3/13   Unclas
17407

University Park, Pennsylvania

Scientific Report 402

Neutral Atmospheric Models Compatible with
Satellite Orbital Decay and Incoherent
Scatter Measurements

by

James Lee Rohrbaugh

November 7, 1972
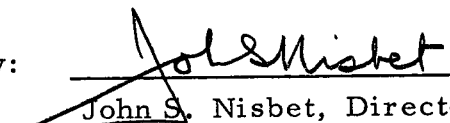
Approved by: _____

John S. Nisbet, Director
Ionosphere Research Laboratory

Ionosphere Research Laboratory

The Pennsylvania State University

University Park, Pennsylvania 16802

ACKNOWLEDGEMENTS

TABLE OF CONTENTS

LIST OF TABLES

LIST OF FIGURES

ABSTRACT

A correlation study has been made of the variations of the exospheric temperature extrema with various combinations of the monthly mean and daily values of the 2800 MHz and Ca II solar indices. A formula incorporating the difference between the daily and monthly average Ca II index and the monthly average 2800 MHz index provided the best fit for all cases tested. The phase and amplitude of the semi-annual component and the term dependent on Kp were found to remain almost the same for the maximum and minimum temperature. The term dependent on the 27 day component of the solar activity was found to be about four times as large for the diurnal maximum as for the minimum.

New observations of T_{max} and T_{min} showed that the ratio of T_{max} to T_{min} is not constant but varies from 1.3 to 1.55 from low to high solar activity. Measurements at Arecibo have also shown that temperature gradient changes at 125 km. are consistent with the phase difference between the neutral temperature and density maxima. This is used to develop an empirical model which is compatible with both the satellite measurements and the available incoherent scatter measurements. A main feature of this model is that day-length is included as a major model parameter.

CHAPTER 1

INTRODUCTION

1.1 General Statement of the Problem

Present models of the neutral atmosphere such as CIRA (1965) and Jacchia (1970) have been derived mainly from satellite orbital decay and falling sphere measurements. Thus, the measured parameter is the neutral density. These neutral density measurements at different times, altitudes, and locations are then related by a family of atmospheric models to a deduced exospheric temperature parameter. Incoherent scatter measurements of the electron and ion temperature and electron density on the other hand can be used to determine the neutral atmospheric temperature directly. Using this technique, it has been found by Nisbet (1967), Carru, Petit, Vasseur, and Waldteufel (1967), and McClure (1969) that major differences between actual temperature measurements and the neutral models based on satellite orbital decay do occur. Up to the present time, little work has been done to develop a model which is compatible with both satellite orbital decay and incoherent scatter measurements.

Present reference atmospheres also use only the variations of the 2800 MHz index to model the solar dependence of the variations of the exospheric temperature. Incoherent scatter measurements have shown only a crude correlation with the 2800 MHz solar index. Prag and Morse (1970) have

found better correlation of solar radiation with the solar calcium plage intensity. It was thought that perhaps two or more indices might be needed to model the effect of the sun on the upper atmosphere since the emissions from the active regions of the sun generally behave differently than those from less active regions and the background radiation.

Furthermore, the neutral models currently being used base their seasonal variations of the diurnal profile of the exospheric temperature on the solar zenith angle. It seems reasonable to expect that these variations should include some function of a daylength parameter. This can be easily understood since the extreme ultraviolet heating in the atmosphere takes place during daylight periods and the loss processes remain quite constant throughout 24 hours.

The object of this study is to develop a neutral atmospheric model which is compatible with satellite orbital decay measurements and incoherent scatter data. An investigation will be made of the correlation with different solar indices, to improve the response to solar EUV changes, and the effect of the daylength parameter on improving the modeling of the seasonal variations in the diurnal profile of the exospheric temperature will be studied.

1.2 Previous Related Studies

1.2.1 Theoretical Studies of the Neutral Atmosphere

The basic relationship between number density, temperature and pressure in an atmosphere composed of an ideal gas was given by Nicolet (1952). This relationship is:

$$\frac{dp}{p} = \frac{dn}{n} + \frac{dT}{T} = -\frac{dz}{H}$$

where $H = \frac{kT}{mg}$ is the scale height. If an atmosphere contains several constituents which are diffusively seperated, then the above equation can be applied to each constituent separately. Using the above formula in conjunction with rocket data, Nicolet (1952) developed a neutral model in which he considered the atmosphere to be in diffusive equilibrium above 160 km. The neutral temperature increased with height up to about 550 km., above which it was constant.

Johnson (1956) studied the effect of thermal conductivity in controlling the temperature distribution of the upper atmosphere and concluded that the atmosphere must be isothermal above approximately 250 km. He also indicated that a very strong positive temperature gradient existed between 100 and 200 km. and that the main heat loss in the upper atmosphere was due to downward conduction rather than radiation.

Nicolet (1959, 1960) also showed that the temperature gradients above 250 km. had to be small. Nicolet (1960) showed that the day to day variations in the neutral temperatures were associated with changes in solar activity since the major heating mechanism was absorption for solar EUV below 200 km. Nicolet then constructed density tables for the isothermal region.

Because the mean molecular mass is not constant in the upper atmosphere, satellite orbital decay data alone can not supply all the parameters needed to completely describe this region. Therefore, a theoretical study by Nicolet (1961) was made to supplement the observational data. Improved methods for calculating such physical parameters as temperature gradients and scale heights were applied as well as introducing the effects of diffusion and heat conduction. This study led to a new set of neutral density and temperature models. The following constant boundary conditions were chosen:

$$T(120 \quad = \quad 324K$$

$$n(N_2, 120) \quad = \quad 5.8 \times 10^{11} \; cm^{-3}$$

$$n(O_2, 120) \quad = \quad 1.2 \times 10^{11} \; cm^{-3}$$

$$n(O, 120) \quad = \quad 7.6 \times 10^{10} \; cm^{-3}$$

These conditions were chosen to ensure that the resulting density at 200 km. would agree with the observed density of about 4×10^{-13} gm cm^{-3}. A complete set of tables of

the resulting densities from 120 to 500 km. as well as reasons for the above choice of boundary conditions was given by Nicolet (1962).

Harris and Priester (1962 a, b, CIRA 1965) developed a time dependent model of the upper atmosphere by solving the following equation:

$$\frac{\partial}{\partial z}\left(k(T)\frac{\partial T}{\partial z}\right) - \rho\, c_p \frac{\partial T}{\partial z}\, T \int_{z_o}^{z} \frac{1}{T^2} \frac{\partial T}{\partial t}\, dz' + Q_{euv} + Q_{ox} + Q' = \rho\, c_p \frac{\partial T}{\partial t}$$

where

$K(T)$	is the coefficient of heat conduction
Q_{euv}	is the heat source due to absorption of the solar EUV – radiation
Q_{ox}	is the heat loss due to infrared radiation of atomic oxygen
Q'	is second heat source

The boundary conditions used were constant in time and were those given by Nicolet (1961) with the exception of the neutral temperature at 120 km. T(120) was taken to be 355 K.

Initially, Q' was not included in the above equation. However, when this term was excluded the solutions to the equation did not agree with observed data. The diurnal maximum in the temperature and density was found to occur at 1700 hours whereas the observed data indicated a maximum at 1400 hours. Furthermore, it was found that a

heating efficiency of 70 to 90 percent would be required
if only EUV radiation heating were considered. Therefore,
Harris and Priester introduced a second heat source, Q',
which had a maximum at 0900 hours and an average magnitude
comparable to the heat provided by the EUV flux. They
proposed that this second heat souce was a result of solar
corpuscular radiation. The need for a second heat source
is apparent in all two dimensional models that do not
include the effects of horizontal transport. The resulting
model given was valid for equatorial and mid-latitudes.

The equation of motion for the atmosphere was solved
numerically by Kohl and King (1966) using the density
model of Jacchia (1965). They showed that the neutral
winds were dependent on the viscosity, Coriolis, and ion
drag forces and were of the order of 100 m sec^{-1} at 300 km.
They proposed that perhaps the second heat source intro-
duced by Harris and Priester (1962) might well be the
neutral winds.

A two dimensional dynamic model of the upper atmo-
sphere was presented by Volland (1967). He included in
his analysis the non-linear terms of the hydrodynamic
and thermodynamic equations of the upper atmosphere.
The system of equations used is as follows:

$$\frac{\partial \rho}{\partial t} + \text{div } (\rho \overline{v}) = 0$$

$$\rho \frac{d\overline{v}}{dt} + \text{grad } p + \text{div } \sigma + \rho \overline{g} = 0$$

$$\rho C_v \frac{dT}{dt} - \text{div} (K \text{ grad } T) + p \text{ div } \overline{v} = q$$

$$P = \frac{R}{M} \rho T$$

where σ is the viscous stress tensor, C is the specific heat at constant volume, K is the coefficient of heat conductivity and q contains the solar EUV input and loss due to infrared radiation. The unknowns in the above equation are ρ the density, p pressure, T temperature, and $\overline{v}$ the wind velocity.

By numerically solving the above system of equations, Volland was able to show that the horizontal component of the wind velocity could replace the artificial second heat source proposed by Harris and Priester (1962). The wind system resulting from the above calculations was horizontal at 600 and 1800 hours with a magnitude of 100 m/s at about 300 km. and vertical at 200 and 1400 hours with a magnitude of 100 m/s above 400 km.

Solving a set of simultaneous partial differential equations for the temperature and the densities, Friedman (1967) constructed a theoretical three dimensional model of the upper atmosphere. The equations used were derived from the equations for conservation of mass, momentum, and energy. Solar EUV and heating caused by hot ambient electrons colliding with the neutral constituents were the only external heat sources included in the analysis. Heat loss due to infrared radiation by atomic oxygen was

neglected. For the equinoctial case, the resulting model yielded a temperature and density maxima that changed in time with increasing altitude. The density maxima changed slowly from about 1600 hours at 200 km. to 1500 hours at 750 km. while the temperature maxima changed from 1530 hours at 200 km. to 1330 hours at 750 km. This gave the model the interesting characteristic that for altitudes above 200 km. the temperature maxima always occurred before the density maxima. For the solstice case, the temperature and density maxima occurred at approximately the same times as in the equinoctral case for each altitude, but the latitudes for the maxima migrated to the north (about 20° N) for the lower altitudes. However, at high altitudes the maxima remained near the equator.

Volland (1969) proposed that a tidal wave propagating up from below 100 km. had a predominant effect on the diurnal variations of the density and temperature below 250 km. A two-dimensional model was calculated using linear perturbation theory. Volland assumed it to be a sufficient approximation below 400 km. He assumed that a tidal wave below which was independent of solar activity and EUV radiative heating which varied in accordance with the averaged 2800 MHz index were the only external heat sources. The calculated model densities agreed rather well with those of Jacchia (1964) above 300 km. and with the observations of Priester at al. (1960), May (1963), Morov (1965, 1968) Taeusch et al. (1968), and King-Hele and Hingston (1967, 1968)

below 250 km. The basic reason for the discrepancy with Jacchia (1964) below 300 km. was that Volland's tidal wave implied that the boundary conditions at 120 km. varied and Jacchia had assumed they were constant.

Friedman (1970) presented a continuation of his earlier studies of 1967. The initial work used a rather coarse grid of points on the globe and as a consequence some skepticism about the conclusions resulted. Therefore, in this later study the mesh of points was refined to bring about more accuracy in the calculations. The physical formulation of the model was also expanded to include global winds. By using several sets of boundary conditions at 120 km., he was able to show that the atmosphere above 200 km. is relatively insensitive to conditions at the lower boundary. The wind calculations indicated that the winds had a maximum of about 100 m/s in the region near 140 km. and decreased in magnitude with increasing altitude. Friedman also showed that the winds had little effect on the density profiles.

In a comprehensive theoretical study, Stubbe (1970) solved ten differential equations simultaneously. The equations solved were the four continuity equations for the ions O^+, O_2^+, NO^+, H^+, the four heat conduction equations for the ions O^+ and H^+, the electrons and the neutral particles, and the two equations of motion for the east-west and north-south neutral wind. His time dependent

solution was good for the height range 120 to 1500 km. Stubbe chose as the lower boundary conditions for the neutral atmosphere the following constant values:

$$T_o = 355 \text{ K}$$

$$n(O_2/120) = 7.5 \times 10^{10} \text{ cm}^{-3}$$

$$n(N_2/120) = 4.0 \times 10^{11} \text{ cm}^{-3}$$

$$n(O/120) = 7.6 \times 10^{10} \text{ cm}^{-3}$$

$$n(He/120) = 3.4 \times 10^{7} \text{ cm}^{-3}$$

Although horizontal motions were accounted for, Stubbe's results showed the late hour maximum of both the temperature and density as did the earlier work of Harris and Priester (1962). He therefore concluded that horizontal winds had practically no effect on the amplitude or phase of the neutral temperature. He then proposed that the phase difference between the neutral temperature and density might be explained by a diurnal variation in the density at the lower boundary. Later, Chandra and Stubbe (1971) showed that this proposition could explain the phase difference. However, Swartz and Nisbet (1971) showed that this phase difference could also be accounted for by keeping the boundary values constant but letting the temperature gradient at 120 km. vary. They reported that such variations in the temperature gradients were actually observed at Arecibo, Puerto Rico.

Recently, Stubbe (1972) showed that the vertical neutral gas velocities in the thermosphere caused by a horizontal wind flux with a non-zero divergence are different for each constituent and therefore subject to frictional forces. He cautioned that once the velocities were modified by frictional forces, the density profiles would no longer correspond to the barometric law. The changes would be such that a decrease in $n(O)$ would correspond to an increase in $n(N_2)$ and vice versa, with changes in composition during magnetic storms being particularly important.

1.2.2 Empirical Models of the Neutral Temperature

As observational data became available, various researchers began to construct empirical models of the upper atmosphere to aid them in the study of this region. One of the first of these models was presented by the Rocket Panel in 1952. It was in tabular form and was nothing more than the weighted averages of several rocket experiments. A constant mean molecular weight of 28.966 g/mole was assumed in reducing the data and data from all seasons, latitudes, and local times were averaged together with no corrections for any of these effects.

Minzer and Ripley (1956) published "The ARDC (Air Force Research and Development Command) Model Atmosphere." They introduced a new temperature parameter T_M, the molecular scale temperature, which was related to the

kinetic temperature T by the following equation.

$$T_M = \frac{T}{M} M_o$$

where M is the mean molecular weight and M_o is the sea
level value of M. The model was in terms of T_M since the
height variation in M was not well known. Later, in 1959,
Champion, Minzner, and Pond revised the earlier 1956 model
as satellite drag data became available. However, both
models had the feature that the temperature gradient
increased with height.

Bates (1959) developed an analytic expression for the
temperature altitude profile. The equation is:

$$T(Z) = T_\infty - (T_\infty - T_o) e^{-T\phi}$$

This expression has a convenient property in that it yields
a simple analytic formula for the density profile when
diffusive equilibrium is assumed above the lower boundary
altitude Z_o. It also has the characteristic where the
temperature rises to an asymtotic value which was needed
to reproduce the isothermal region of the upper atmosphere
which was proposed by Johnson (1956).

Jacchia (1960) developed an empirical formula to
describe the densities deduced from early satellite drag
data. The model was a function of the 20 cm solar flux
and assumed the diurnal bulge to be at the same latitude
as the sub-solar point but lagging in time by some fixed
amount.

Jacchia (1964) produced the first of his "static diffusion" models. He assumed the temperature profile had the following form:

$$T(Z) = T_\infty - T(120)) \exp [-s(Z-120)]$$

which is similar to the profile proposed by Bates (1959). S was given by the following function of T:

$$S = 0.0291 \exp (- \frac{X^2}{2})$$

where

$$X = \frac{T_\infty - 800}{750 + 1.722 \times 10^{-4} (T_\infty - 800)^2}$$

Given in terms of the exospheric temperature, density tables were constructed which fitted both the available satellite drag data and the assumed temperature profile. Constant boundary conditions at 120 km. were assumed. The exospheric temperature was given by empirical formulae which accounted for variations with the solar cycle, variations within one solar rotation, semi-annual variations, diurnal variations, and geomagnetic effects. The coefficients for the empirical formulae were later revised (Jacchia, 1965, 1967) as new data was obtained.

Stein and Walker (1965) presented a simple analytic model of the upper atmosphere. They fitted the Bates (1959) profile to the satellite drag data of King-Hele (1963). By doing this, they were able to show that they could reproduce the observed density profiles for a wide range

of boundary conditions at 120 km., thus demonstrating that satellite drag data alone are insufficient to determine atmospheric conditions at the boundary altitude. They also found that for a given value of $n(N_2/120) + n(O_2/120)$, the value of T_∞ depended principally on $n(O/120)$ and was nearly independent of $T(120)$ while the value of τ depended principally on $T(120)$ and was nearly independent of $n(O/120)$.

Realizing that both the temperature and density at 120 km. do vary, Jacchia (1970 a) tried to improve on his 1965 model by moving the lower boundary to 90 km. The assumed temperature profile starts from a constant $T_0 = 183$ K at $Z_0 = 90$ km., with a gradient $G_0 = (dT/dz)\big|_{Z = Z_0} = 0$. The temperature then rises to a fixed inflection point at $Z_x = 125$ km. and eventually increases to an asymptotic temperature T_∞. T_x and G_x, the temperature and temperature gradient at Z_x, are functions of the exospheric temperature and specified by:

$$T_x = a + b\, T_\infty + c \exp(\overline{k}\, T_\infty)$$

$$G_x = \left.\frac{dT}{dz}\right|_{z = z_x} = 1.9 \frac{T_x - T_o}{z_x - z_o}$$

where a, b, c, $\overline{k}$ are constant coefficients. The complete temperature profile is given by:

$$T(z) = \begin{cases} T_x + \sum_{m=1}^{4} C_m (Z - Z_m)^m, & Z_o < Z < Z_x \\ T_x + A \tan^{-1}\left\{\frac{G_x}{A}(Z - Z_x)[1 + B(Z - Z_x)]^n\right\}, & Z > Z_x \end{cases}$$

The coefficients A, B, N, G_x, and C_m are adjusted to fit the related densities to the observational data.

The density tables were later revised (Jacchia, 1970 b) in such a manner to become much larger. As in the earlier model (Jacchia, 1964), the exospheric temperature was modeled with empirical functions which included all the variables included in his earlier work.

Carru and Walteufel (1969) and Waldteufel (1970) derived similar empirical functions for the exospheric temperature from incoherent scatter data taken at St. Santin - Nançay, France. The empirical functions differed from those given by Jacchia (1965). Waldteufel (1970) was able to explain these differences on the basis of the variable boundary conditions at 120 km. used in his analysis. The boundary conditions were allowed to vary according to observed data from the incoherent scatter measurements.

The latest empirical model of the neutral atmosphere is given by Jacchia (1971 a). The basic format of the model is the same as his 1970 model with one major change. On reanalyzing the density variations obtained from orbital drag data in the interval 1958 to 1970, Jacchia (1971 b) found that the amplitude of the semi-annual density variation did not seem to be related to solar activity. He therefore proposed a correction factor for the semi-annual density variation that is only a function of time and altitude. This correction is added to the total density and takes the form:

$$\log_{10} \rho_{semi-annual} = f(Z) \, g(t)$$

where

$$f(Z) = (5.876 \times 10^{-7} \, Z^{2.331} + 0.06328)$$
$$\cdot \exp(-2.868 \times 10^{-3} Z) \quad (Z \text{ in km})$$

$$g(t) = 0.02835 + 0.3817 \left[1 + 0.4671 \sin(2\pi \, \tau + 4.137) \right]$$
$$\cdot \sin(4\pi \, \tau + 4.259)$$

$$\tau = \Phi + 0.09544 \left[\frac{1}{2} + \frac{1}{2} \sin(2\pi \, \Phi + 6.035) \, 1.650 - \frac{1}{2} \right]$$

$$\Phi = (Z - 36204)/365.2422$$

t = time expressed in Modified Julian Days (MJD = Julian
    Day minus 2,400,000.5)

This correction factor makes the model difficult to use
since there is no apparent way of applying the semi-annual
variation to the densities of each individual constituent
without destroying the diffusive equilibrium assumption.

1.2.3 Previous Studies of the Various Solar Indices

An index that is well correlated with the neutral
atmospheric temperatures and ionizing radiation is of great
importance when relating ionospheric or neutral atmospheric
measurements to other data obtained under different condi-
tions of solar activity. Several comparisons have been
made between the various ground based indices and the EUV
fluxes. Hall et al. (1969) compared nine EUV line
intensities with the daily average 2800 MHz flux over a
period from 1961 to 1968. Prag and Morse (1970) showed
that short term fluctuations in three EUV bands were better

correlated with an index based on the sum of the products of the calcium plage areas, intensities, and cosines of their angular distances to the central meridian, than with the 2800 MHz solar flux. Timothy and Timothy (1970) compared the intensity of the 304 $\overset{o}{A}$ line over several months with the 2800 MHz solar flux, the Zurich relative sunspot number, and the McMath calcium plage area. They concluded that the 304 $\overset{o}{A}$ intensity was poorly correlated with these ground based indices, but that the Zurich sunspot number was the best, and the calcium plage area the poorest of the three. Woodgate et al. (1972) made a similar comparison for four wavelengths using six months of OSO VI data. They found that the correlation coefficients for the 304 $\overset{o}{A}$ intensity were 0.83 with the 2800 MHz flux and 0.73 with the Zurich sunspot number. Later, Dr. Woodgate in conjunction with Nisbet, Swartz and Rohrbaugh (1972), found a correlation factor of 0.82 between the 304 $\overset{o}{A}$ intensities and the Ca II index involving the area, intensity, and angle between the plages and the center of the solar disk.

The relationship between the ground based indices and the exospheric temperatures is less direct than with the EUV fluxes. The energy input of the different wavelength groups depends on various factors such as the photon energy, photon flux and atmospheric cross section. The temperatures are controlled by energy storage and transport as well as by the energy input. Therefore, Nicolet (1963)

studied the variation of the average temperatures deter-
mined from satellite orbital decay density measurements
with various frequencies in the range from 1000 MHz to
10,000 MHz. He concluded that the 3750 MHz intensity was
a better modeling index than the 2800 MHz intensity.
Presently, neutral atmospheric models such as CIRA (1965)
and Jacchia (1971) use the 2800 MHz index to model the
variations with solar activity.

1.3   Specific Statement of the Problem

1.3.1   Compatibility of Satellite Orbital Decay Data and Incoherent Scatter Temperatures

Can satellite orbital decay data be made compatible
with temperatures deduced from incoherent scatter measure-
ments by making appropriate changes in the temperature
gradient at 120 km?

1.3.2   Inclusion of a Daylength Parameter into the Exospheric Temperature Model

Should the seasonal variations in the diurnal profile
of the exospheric temperature model be a function of a
daylength parameter rather than being tied to the subsolar
point as is presently the case?

1.3.3   Relative Usefulness of the Calcium Plage and Monthly Mean 2800 MHz Indices in an Empirical Model

Can the calcium plage intensities provide a better
index for the fluctuations of the exospheric temperature
extrema to solar EUV radiation changes than the 2800 MHz
index? Should more than one index be used?

CHAPTER 2

METHOD OF ANALYSIS

2.1 Determining the Exospheric Temperature

Swartz and Nisbet (1971) have shown that a consistent neutral model could be developed using incoherent scatter data from Arecibo. The method used to determine the exospheric temperatures was first to calculate the neutral temperatures from the electron and ion temperatures using the ion thermal balance technique as described by Nisbet (1967). The entire temperature profile was then used in a least squares fit of the Bates formula (1959) given in equation (1). The neutral densities were adjusted with the temperature profiles to ensure that a valid diffusive equilibrium model resulted.

$$T(Z) = T_{\infty} - \{T_{\infty} - T_{o}\} e^{-\tau\phi} \qquad (1)$$

where:

$T(Z)$ = neutral temperature at altitude Z

T = exospheric temperature

T_{o} = neutral temperature at lower boundary

τ = shape parameter

ϕ = geopotential altitude given by

$$\phi = \frac{(Z - Z_{o})(R + Z_{o})}{R + Z}$$

R is the radius of the earth, and Z_{o} is the altitude of the lower boundary.

This process of fitting entire profiles can be long and tedious. Therefore, a quicker and easier way of determining the exospheric temperatures was sought.

If one assumes that Jacchia's densities (1970) are correct, the neutral exospheric temperature can be calculated directly from incoherent scatter data by using Nisbet's (1967) technique which assumes that the energy input to the ions is equal to the energy loss. When the energy transfer rates of Banks (1966 a, b) are adopted and assuming only atomic oxygen ions, the following equations apply,

$$Q_{ei} = \frac{4.8 \times 10^{-7} \, N_e \, N(O^+) \, (T_e - T_i)}{T_e^{3/2}} \tag{2}$$

$$Q_{in} = 0.21 \times 10^{-14} \, n(O^+) n(O) (T_i + T)^{1/2} (T_i - T)$$

$$+ \, 6.6 \times 10^{-14} \, n(O^+) n(N_2) (T_i - T)$$

$$+ \, 5.8 \times 10^{-14} \, n(O^+) n(O_2) (T_i - T) \tag{3}$$

where

N_e is the electron density

T_e is the electron temperature

T_i is the ion temperature

$N(O^+)$ is the atomic oxygen ion density

$N(O)$ is the atomic oxygen density

$N(N_2)$ is the molecular nitrogen density

$N(O_2)$ is the molecular oxygen density

T is the neutral temperature

By equating equations (2) and (3) and rearranging, one gets equation (4) which was then used to calculate the daytime temporal variation of the neutral temperature.

$$T = T_i - \frac{4.8 \times 10^7 \, N_e (T_e - T_i)}{T_e^{3/2} \{6.6n(N_2) + 0.21(T_i + T)^{1/2} \, n(O) + 5.8n(O_2)\}}$$

(4)

Each temperature was then extrapolated upward following the assumed profile shape of equation (1) and averaged to provide the exospheric temperature through

$$T_\infty = \frac{\sum_i W_i \left\{ \frac{T(z_i) - T_o \, e^{-\phi_i}}{1 - e^{-\tau\phi_i}} \right\}}{\sum_i W_i}$$

(5)

where the W_i are weighting functions based on the uncertainties introduced into T_∞ by the various parameters in each extrapolation.

To determine the nighttime exospheric temperature, the assumption was made that

$$T_e = T_i = T$$

This assumption seems reasonable because the electron and ion temperatures are observed to be very close to one another and the calculated energies given by the electrons to the ions should not result in a significant ion-neutral temperature difference. Again each neutral temperature was extrapolated upwards and averaged using equation (5). In

this manner, the diurnal variation of T_∞ was determined

for many days at Arecibo.

2.2 Deriving an Empirical Function of T_∞

Approximately 20 sets of exospheric temperatures

covering periods of at least 24 hours were obtained and

normalized according to:

$$T_{norm}(t) = \frac{T_\infty(t) - T_{min}}{T_{max} - T_{min}} \qquad (6)$$

where:

$T_{norm}(t)$ = normalized exospheric temperature

as a function of time

T_{min} = diurnal minimum exospheric temperature

T_{max} = diurnal maximum exospheric temperature

Then all sets in a particular season were averaged together.

These averaged normalized, diurnal variations are shown in

Figure 1, which compares them with the constant shape of

the Jacchia 1970-35c model. Winter and summer curves for

three incoherent scatter stations are compared in Figures

2 and 3.

Examination of Figures 1 through 8 showed that the

timing of the diurnal minimum and maximum not only varied

with season but that the shift corresponded with the varia-

tion in daylength. This implied that the seasonal changes

in the normalized diurnal variations should be based on

day length as well as the solar zenith angle at noon. Since
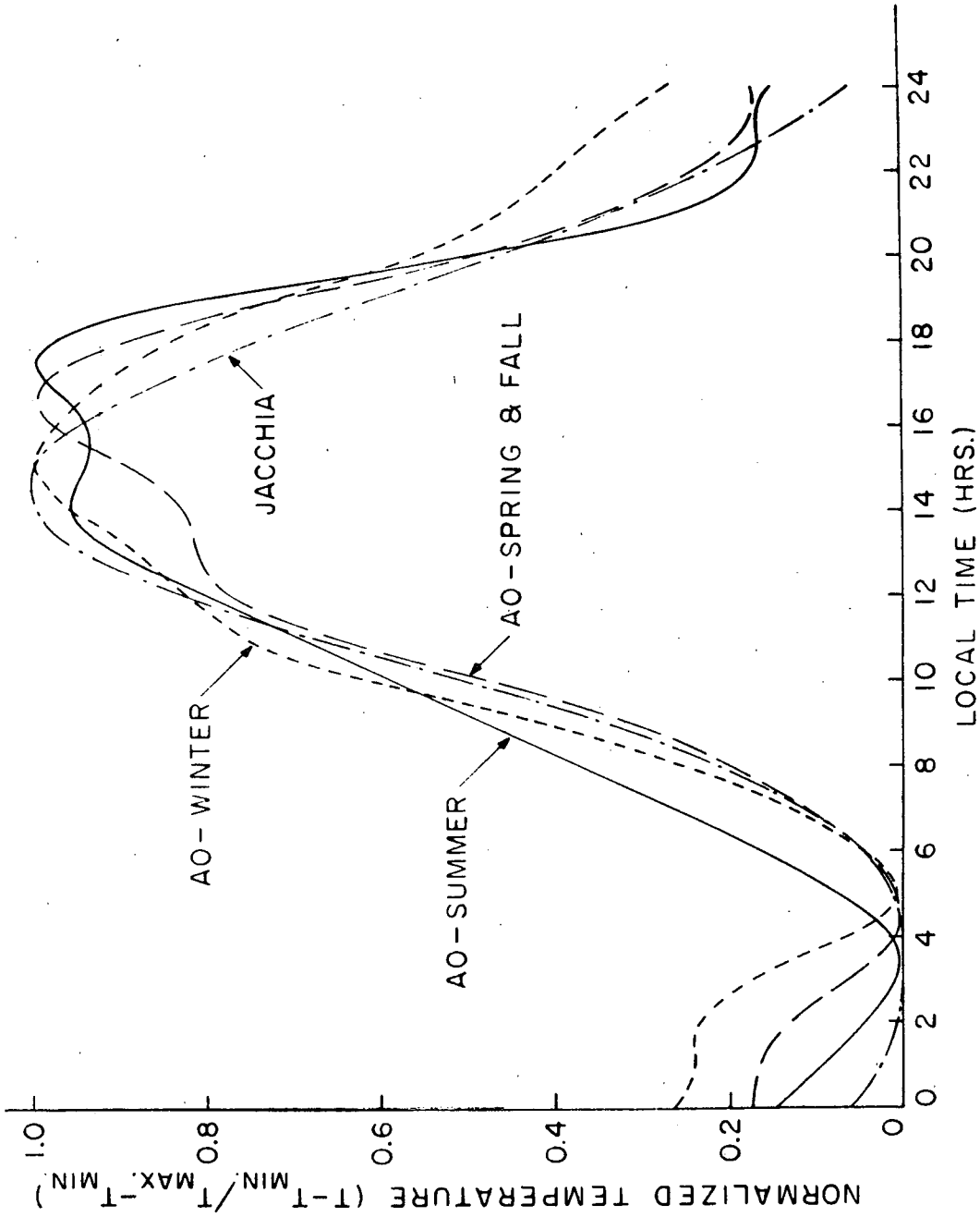
FIGURE 1: Seasonal Variation of the Normalized Exospheric Temperature at Arecibo and that of the Jacchia (1970-35C) Model.
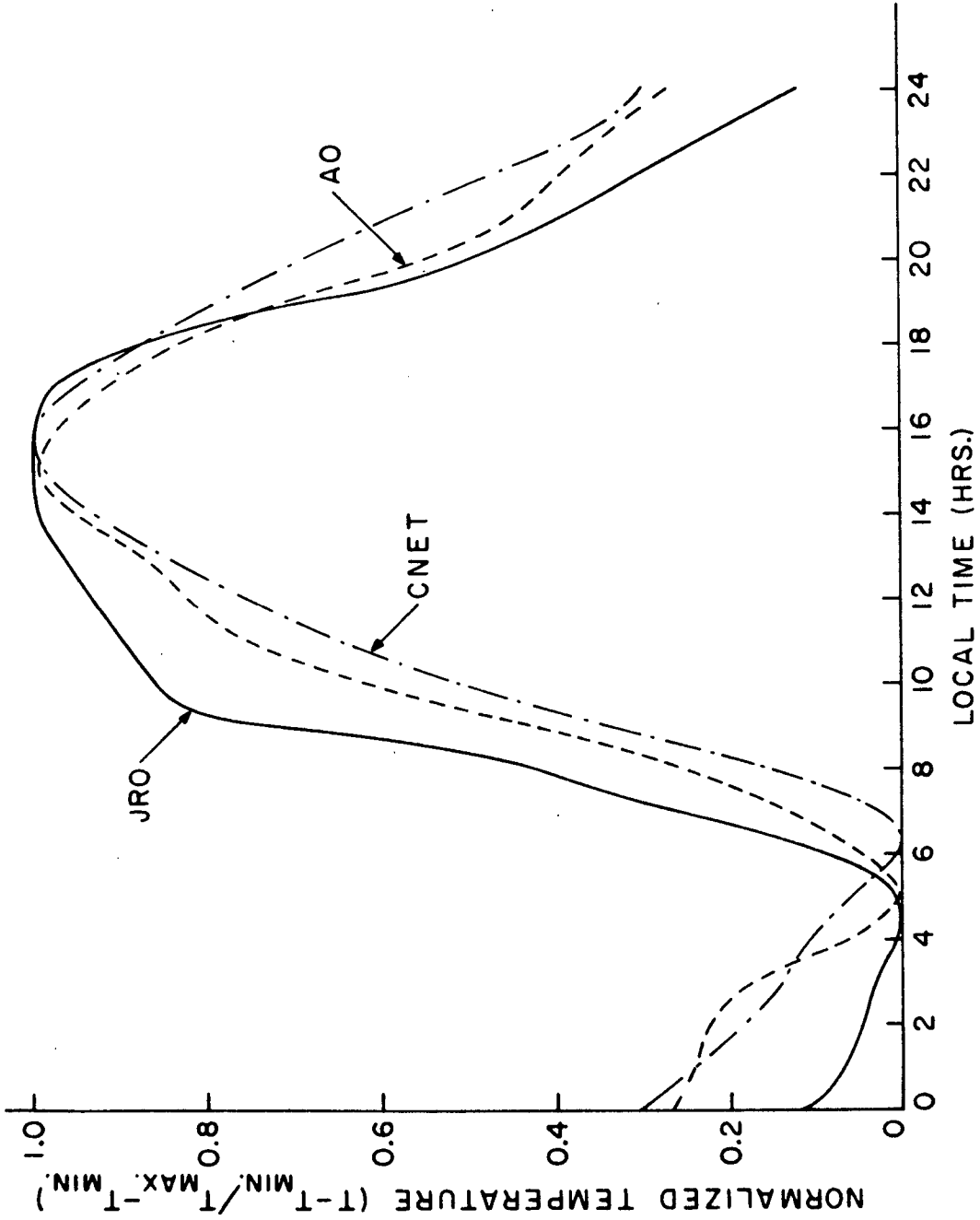
FIGURE 2: Winter Diurnal Variation of the Normalized Exospheric Temperature.
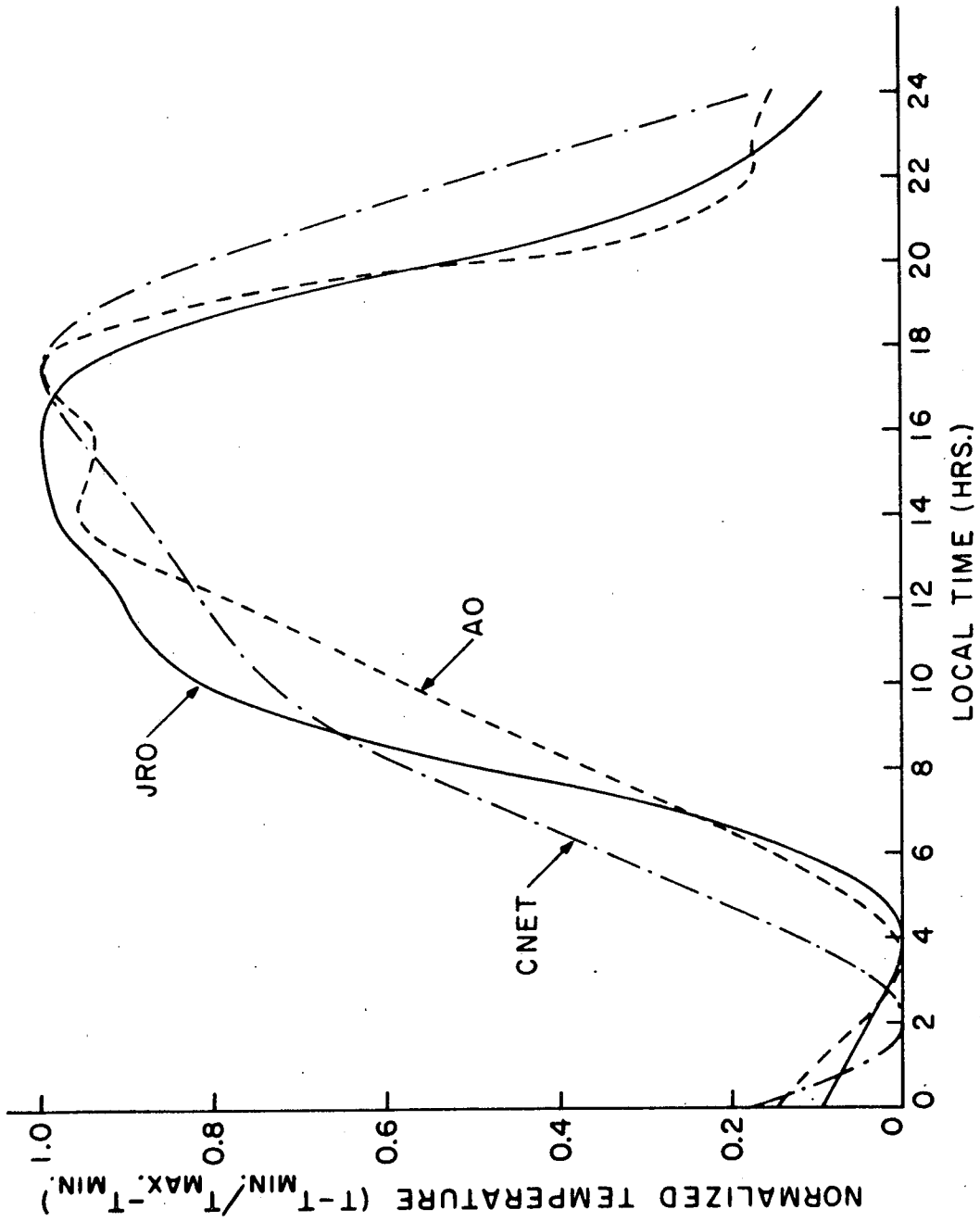
FIGURE 3: Summer Diurnal Variation of the Normalized Exospheric Temperature.

the EUV input should be greater than the energy conducted downwards during the day and less during the night, the maximum in the absence of winds would occur at sunset and the minimum at sunrise. This effect is somewhat like a non-linear capacitor charging up through the day and discharging through the night. In reality the maximum is shifted to a time earlier than sunset by the global wind system. It would be expected that the time before sunset would be more important than the distance from the subsolar point used in present models.

To model this effect, each 24 hour period was Fourier analyzed and then normalized in the manner previously described. These normalized Fourier coefficients were then averaged according to season and finally fitted to a function of daylength.

2.3 Analyzing the Diurnal Maximum and Minimum Exospheric Temperature

Current neutral atmospheric models use a combination of the 2800 MHz solar flux index, $S_{10.7}$, and the average 2800 MHz flux, $\overline{S}_{10.7}$, to model the effects of solar EUV radiation on the upper atmosphere. These models use the average flux to describe the effects of the background radiation from the sun and use the difference between the average flux and the flux for a given day to describe the effects of the active regions. It has been shown recently by Prag and Morse (1970) that a better correlation

exists between the fluctuations of certain bands of solar
EUV radiation measured by the Spades satellite and the
solar calcium plage intensities than with the 2800 MHz
index. If this is true of the solar EUV radiation which is
absorbed in the upper atmosphere, then it was felt that the
calcium plage intensity should also provide a better index
for models of the exospheric temperature. Both the 2800
MHz index and the calcium index were studied to decide
which would best model the variations in the diurnal
maximum and minimum exospheric temperatures.

The calcium plage indices were constructed from the
tables in "Solar Geophysical Data" which give the location,
area and intensity of each plage as recorded at the McMath-
Hulbert Observatory. The index was found by summing the
products of the area, intensity and cosine of the angular
distance from each plage to the center of the solar disk.
These indices from 1958 through 1970 can now be found in a
report by Swartz and Overbeek (1971) and in "Solar Geophysi-
cal Data" from December, 1971 on. The values given by
Swartz and Overbeek must be divided by 1000 to be compatible
with those in "Solar Geophysical Data."

The plage intensities used to calculate the Ca II
index are related to the brightness of the solar disk so
are essentially normalized to 1 A.U. To take care of the
variation in the sun earth distance a modified Ca II index
was used.

$$Ca\ II = Ca^*II\left(\frac{R_o}{R}\right)^2 = \frac{Ca^*II}{\{1.0-0.01676\ \cos\ [(D-5)\ \frac{2\pi}{365.25}\ ]\}^2}$$

where

Ca II is the unnormalized calcium II index.

Ca^*II is the normalized calcium II index given in "Solar Geophysical Data" or 10^{-3} times the index given by Swartz and Overbeek (1971).

D   is daynumber of year counting from 1 January.

The behavior of the calcium plage index for 1967 is shown at the top of Figure 4 as compared with the 2800 MHz index given in the lower graph. From this it can be noted that both indices have the same basic period as the solar rotation period, about 27 days, but that the calcium plage index has a greater percentage change than the 2800 MHz index. Also there are periods when the 2800 MHz index remains relatively constant when compared to the calcium II index.

Other differences between these two indices are noted in Figure 5. It can be seen that the general relationship between the two indices appears to be non-linear. In addition, it shows that when the calcium II index tends to zero, the 2800 MHz index is about 75.

Since the calcium II index depends on the relative brightness of plages given by visual inspection of the solar disk where as the 10.7 cm index is a measured value, the random noise in each parameter had to be investigated.
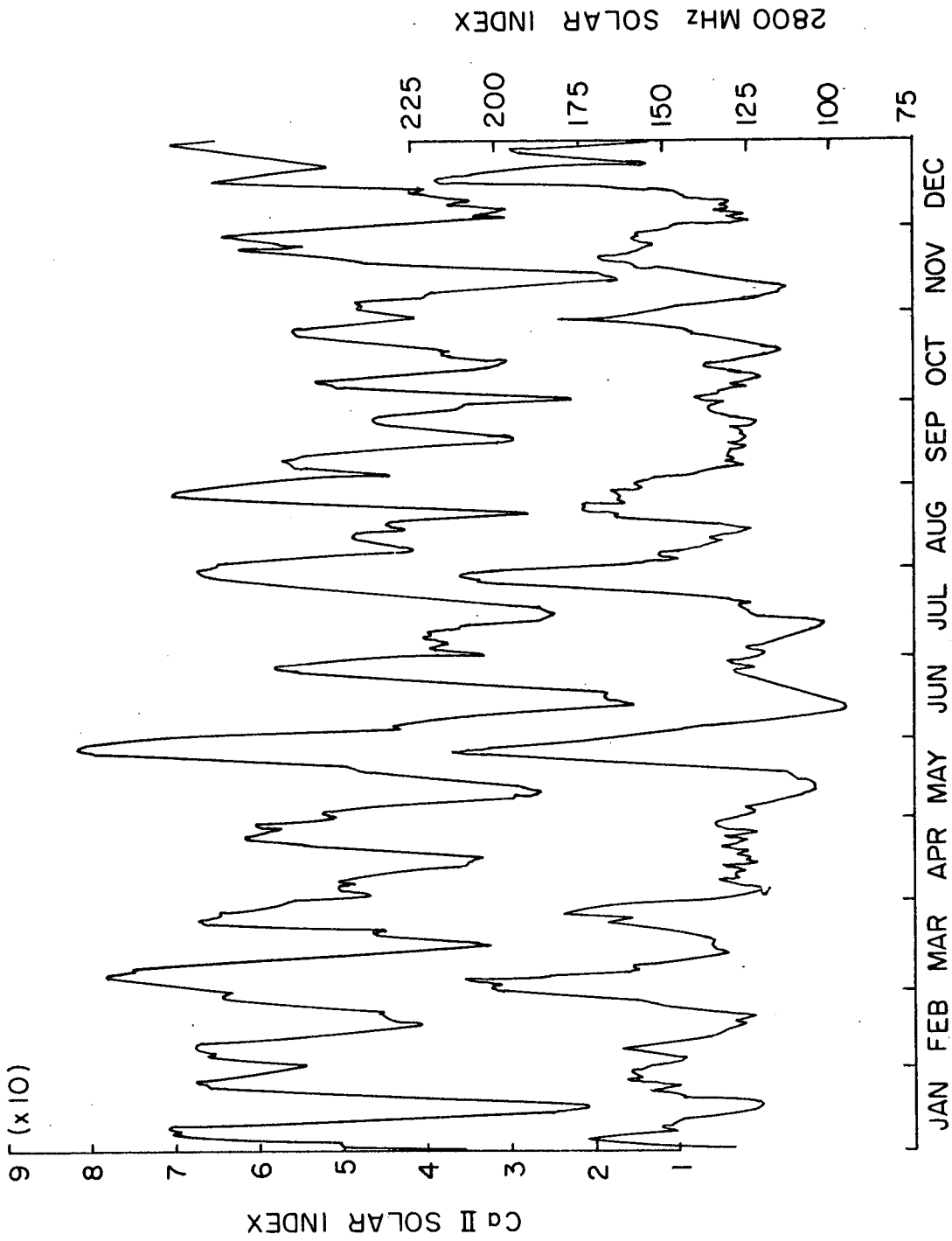
FIGURE 4: Behavior of the Ca II and 2800 MHz Solar Indices for 1967.
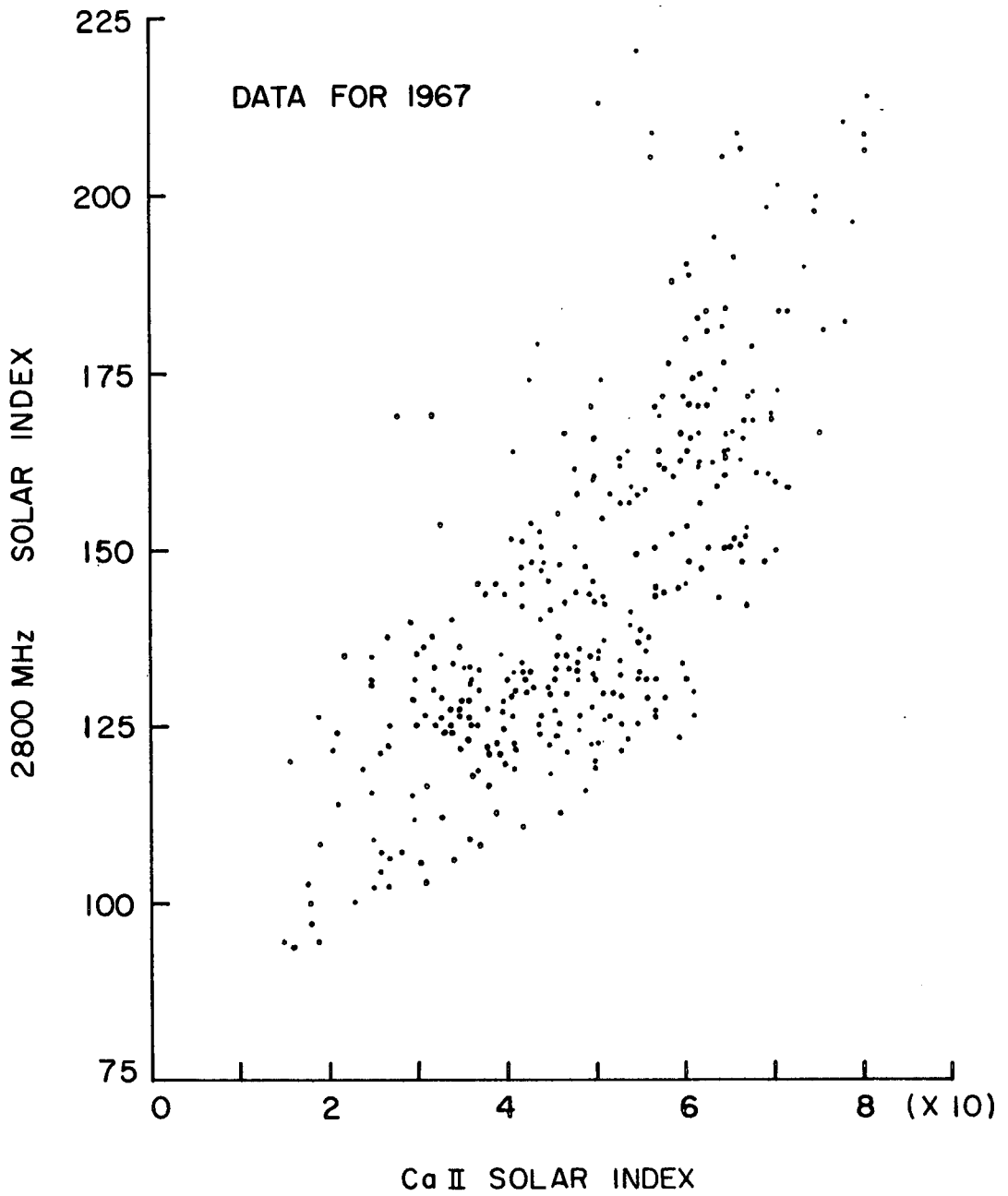
FIGURE 5: 2800 MHz Index Vs. Ca II Index for 1967.

The autocorrelation function of each index was used to make
an estimate of this random noise. These functions were
calculated using data from 1958 through 1970 and are
shown in Figure 6. The eleven year solar cycle is evident
in both indices and the 27 day solar rotation period can
be seen superimposed on it. Figure 7 shows the autocorre-
lation functions with the eleven year solar cycle removed.
It can be seen that the noise bandwidth for both indices
are nearly the same and approximately equal to the recipro-
cal of the solar rotation period. This figure also shows
that the correlation time for each index is of the order
of 5 days. These correlation times give some idea of the
time scales of atmospheric changes which can be correlated
with these indices. Since the time constant of the upper
atmosphere is of the order of a day, both indices should,
in this respect, be of equal value in describing the
response of the upper atmosphere to solar EUV changes.

A more quantitative approach to the relationship
between the two indices is given by the cross correlation
function. When the eleven year component of both indices
was included, the correlation factor was calculated to be
about 0.9. It was felt that this large correlation factor
was due to the fact that the eleven year components of both
indices were in phase. Since the time period of interest
in the upper atmosphere are at most of the order of day,
the eleven year components were removed and the cross
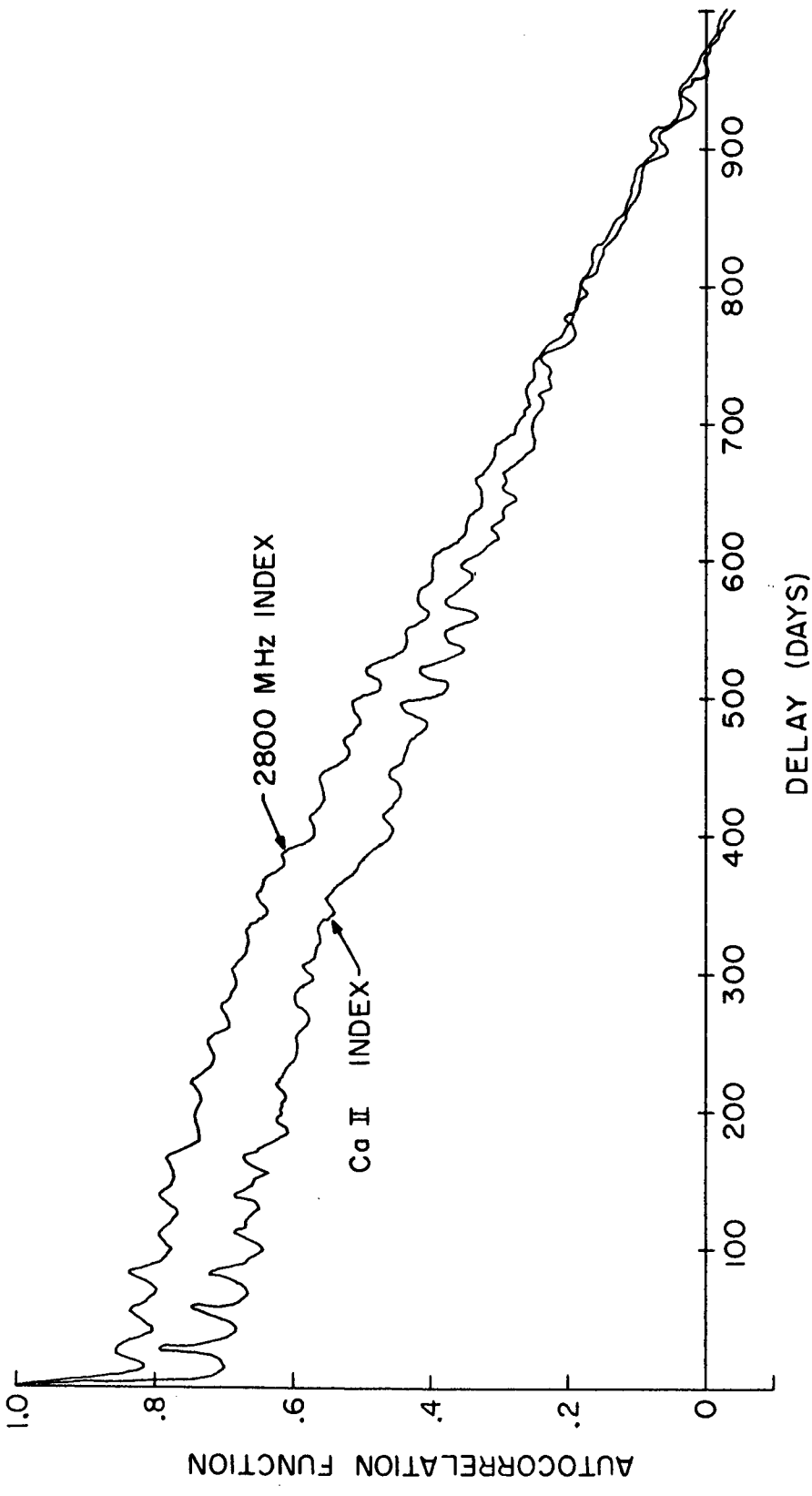
FIGURE 6: Autocorrelation Functions for the Ca II and 2800 MHz Indices.
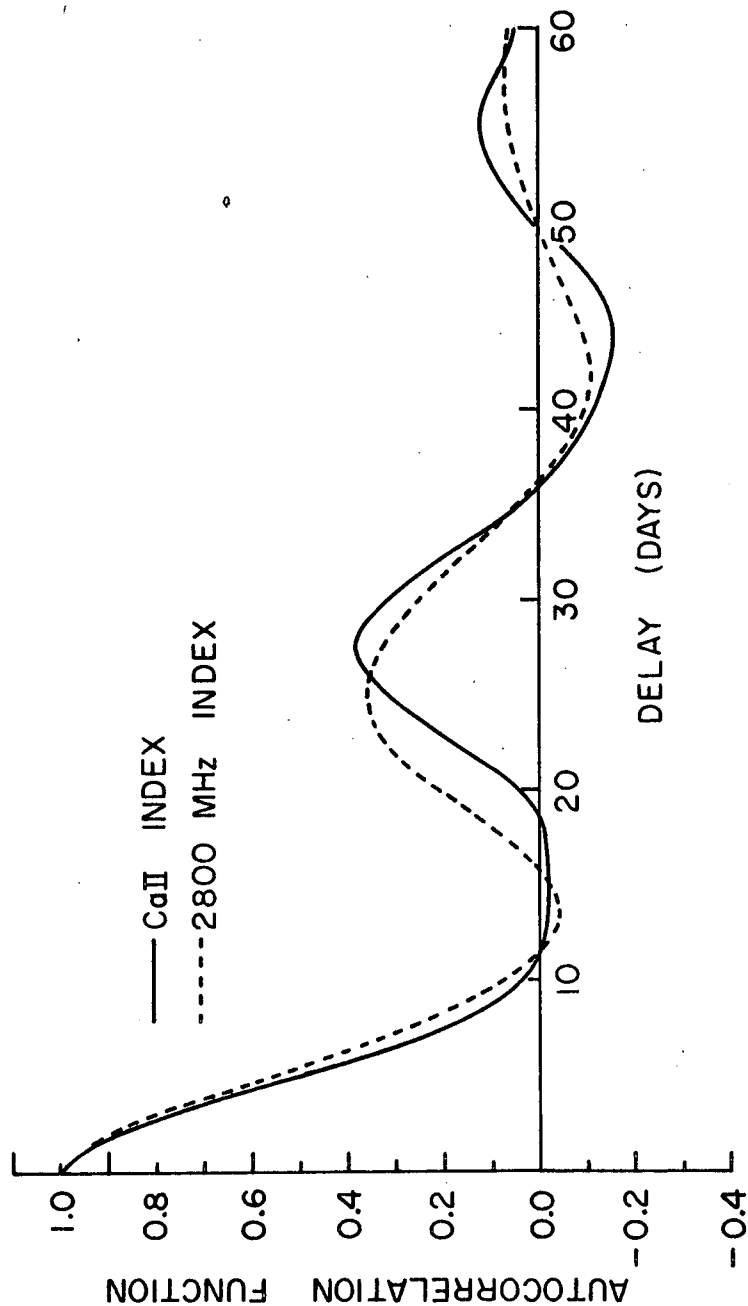
FIGURE 7: Autocorrelation Functions for the Ca II and 2800 MHz Indices with the Eleven Year Component Removed.

correlation function was recalculated in an effort to get a correlation factor for a shorter time scale.

Figure 8 is a graph of this short term cross correlation. When the long term components were removed, the correlation factor was reduced to about 0.7.

Because both indices did have distinct properties, it was important to determine which index was best suited for modeling the exospheric temperature extrema. The data used for this analysis were 20 sets of diurnal maximum and minimum exospheric temperatures deduced from incoherent scatter measurements in the manner described in section 2.1. These temperature extrema were evenly distributed over the period from January 1967 to June 1969, during which time the 2800 MHz index varied from 100 to 180 x 10^{-22} watts m^{-2} Hz^{-1}.

In addition to the above incoherent scatter data, approximately 850 diurnal minimum exospheric temperatures were derived from values of the half-thickness of a parabola (SCAT) given for Ramey, Puerto Rico in "Solar Geophysical Data" for 1 November 1959 through 31 March 1962. Assuming a Chapman C_α form for the peak of the F-layer at night allows these values to be converted to temperatures assuming atomic oxygen as the major ion and equilibrium of the electron, ion and neutral temperatures. In this work it has been assumed, following Quinn and Nisbet (1965), that:

$$T_\infty = 21.0 \text{ SCAT}$$
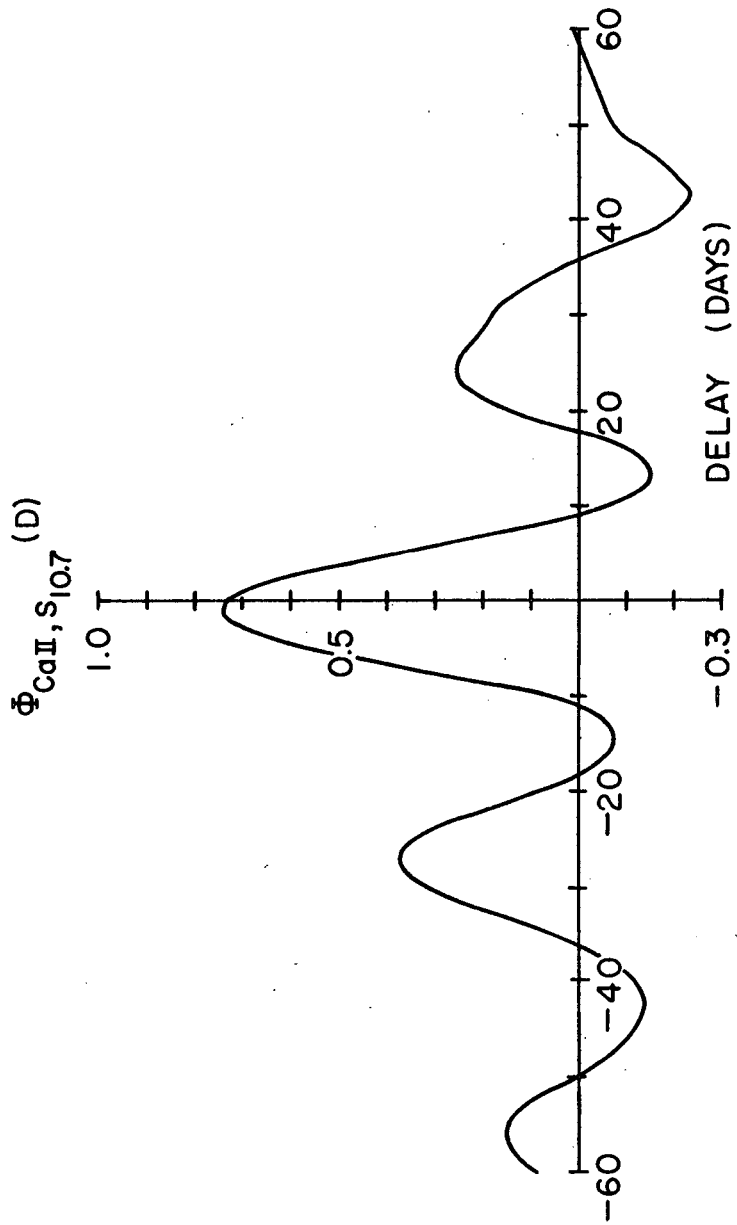
FIGURE 8: Cross Correlation Function of the Ca II and 2800 MHz Indices without the Eleven Year Component.

where T_∞ is the exospheric temperature in Kelvin and SCAT is given in kilometers. The 2800 MHz index varied from 74 to 252 x 10^{-22} watts m^{-2} Hz^{-1} during this period.

A series of fits was made to these temperatures using several combinations of the solar indices as well as several functional forms. The RMS error for each function and solar index was then compared to decide upon the final form. After having picked a function, which was valid only for Arecibo, it was then expanded as a function of daylength so that it could be used in a global model.

2.4 Boundary Conditions

Although there is strong indication of variable conditions at 120 km., little is yet known about the detailed structure or dependencies of the variations. Hence, for the form of the model presented here, the following constant boundary conditions were assumed:

$$Z_o = 120 \text{ km.}$$

$$T_o = 400 \text{ K}$$

$$N(N_2, Z_o) = 4.0 \text{ x } 10^{11} \text{ cm}^{-3}$$

$$N(O, Z_o) = 9.33 \text{ x } 10^{10} \text{ cm}^{-3}$$

$$N(O_2, Z_o) = 5 \text{ x } 10^{10} \text{ cm}^{-3} \tag{7}$$

The boundary temperature given here is somewhat higher than indicated in the present models, but is the average value found by Swartz and Nisbet (1971) at Arecibo.

2.5 Calculation of τ and Fitting the Temperature Gradient at 120 km.

At this point, all the parameters of the assumed profile given in equation (1) has been modeled independently except the profile shape parameter, τ. Assuming diffusive equilibrium above Z_o, the lower boundary this type temperature profile yields the following density formulation.

$$N(j, z) = N(j, z_o) e^{\tau \phi} \left\{ \frac{T_o}{T_\infty (e^\phi - 1) + T(Z)} \right\}^{1 + \gamma_j} \qquad (8)$$

where

$$\gamma_j = \frac{M_j \, g_o}{\tau \, k T_\infty}$$

g_o = accelaration of gravity at Z_o

M_j = mass of the yth constituent

k = Boltzman's constant

Solving for τ gives

$$\tau = \frac{\ln \left\{ \frac{T(Z)}{T_o} \right\}}{\frac{T_\infty \, k}{M_j \, g_o} \ln \left\{ \frac{n(j, \, Z_o) \, T_o}{N(j, \, Z) \, T(Z)} \right\} - \phi} \qquad (9)$$

This equation combines the exospheric temperatures deduced from incoherent scatter data with the density measurements of satellite orbital decay, thus reconciling the two empirically. In the present case, the atomic oxygen

densities from Jacchia's 1970-35c model was used with the
Arecibo data.

Using an iterative technique involving equations (1)
and (9), a τ was calculated for each measured value of T_∞.
The initial value of T(300) was chosen to be T_∞. However,
this iterative process did demand certain restrictions
to ensure that a $\tau > 0$ would result.

To ensure a positive τ , the denominator of equation
(9) must be positive. Hence:

$$T_\infty \qquad \frac{m_j \; g_8 \; \phi}{k \; \ln \left\{ \dfrac{N(j, \; Z_o) \; T_o}{n(j, \; Z) \; T(Z)} \right\}} \qquad (10)$$

Since the following inequalities hold for $Z > Z_o$,

$$T_\infty > T(Z) > T_o$$

$$N(j, \; Z_o) > N(j, \; Z)$$

$$N(j, \; Z_o) \; T_o > N(j, \; Z) \; T_\infty > N(j, \; Z) \; T(Z)$$

it follows that

$$\ln \left\{ \frac{N(j, \; Z_o) \; T_o}{N(j, \; Z) \; T_\infty} \right\} \quad < \quad \ln \left\{ \frac{n(j, \; Z_o) \; T_o}{N(j, \; Z) \; T(Z)} \right\}$$

Since equation (10) requires an apriori knowledge of τ ,
a more practical test of the compatibility of the exospheric
temperature with the other data is:

$$T_\infty > \frac{M_j \, g_o \, \phi}{k \, \ln \left\{ \frac{N(j, \, Z_o) \, T_o}{N(j, \, Z) \, T_\infty} \right\}} \tag{11}$$

This is a more stringent requirement and if satisfied, equation (10) will always be satisfied also.

Since the neutral temperature at 300 km. is generally quite close to the exospheric temperature, the simple use of equation (10) does not place too severe a restriction on the model of T_∞.

After a set of τ's for each temperature data block were obtained, they were then used to calculate the temperature gradients at 120 km. using equation (12).

$$\left. \frac{dT(Z)}{dZ} \right|_{Z \, = \, 120} = \tau \, (T_\infty - T_o) \tag{12}$$

Each set of temperature gradients that covered a period of at least 24 hours was then Fourier analyzed after being grouped according to season. The Fourier coefficients obtained for each season were then analyzed to get a simple model of the temperature gradient.

CHAPTER 3

RESULTS OF THE ANALYSIS

3.1 Results of the Correlation Study

A series of fits was first made to the diurnal tempera-
ture extrema deduced from incoherent scatter measurements
using the simple function:

$$T = a + b \ I(t - d) \qquad\qquad (13)$$

where I was either the calcium II index or the 2800 MHz
index. d was varied from 0 to 27 to allow for a time lag
between the temperature measurement at Arecibo and the
index measurement.

The RMS errors in the fits for each delay were then
examined. Figure 9 shows the results of this analysis for
both the maximum and minimum exospheric temperatures. The
upper graph is for the maximum temperature. This shows that
the calcium II index does give a significantly better fit
than the 2800 MHz index. The minimum error occurred for
the Ca II index three days prior to the given temperature
measurement.

The lower graph gives the results for the diurnal
minimum temperatures. Here, again, the Ca II index gives
a better fit. However, it is interesting to note that the
general level of the correlation of these temperatures is
much poorer than for the maximum temperatures. That is,
the RMS error barely dips indicating only a slight
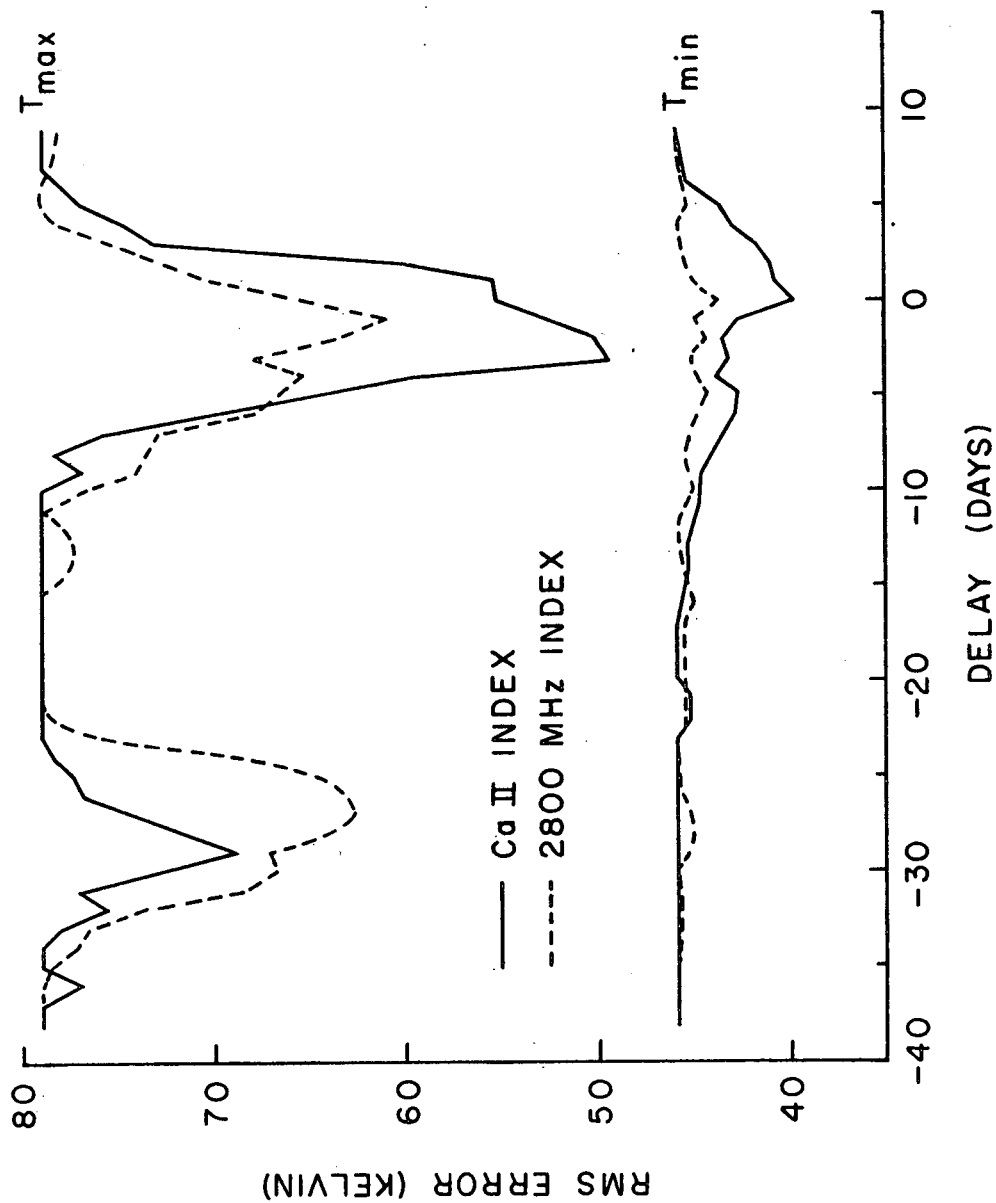
FIGURE 9: Variation of the Root Mean Squared Error for Linear Fits to the Maximum and Minimum Temperatures with Variable Time Delays for the Ca II and 2800 MHz Solar Indices.

correlation. This poor correlation with both indices in conjunction with the fact that the minimum temperatures are not very small could indicate that long wavelength radiation which is absorbed in the lower atmosphere and controls the temperature gradients in the lower thermosphere is not greatly dependent on solar activity or that other heat sources not well correlated with the day to day changes in solar activity are controlling the nighttime minimum temperatures.

A non-linear least squares fitting program was then used to fit various functions to the complete data set. The general form of the equation used was:

$$T = G_1 + G_2 X + G_3 K_p + G_5 \, \text{Sin} \, (\frac{4\pi D}{365.25} + G_4) + G_6 \, Y$$

$$(14)$$

where T was either the maximum or minimum exospheric temperature, X was either $(S_{10.7} - \overline{S}_{10.7})$ or $(Ca - \overline{Ca})$ and Y was either $\overline{S}_{10.7}$ or $\overline{Ca}$. Using the various combinations of solar indices possible in the above equation, a series of fits was made allowing for a delay between the index measurement and the temperature measurement.

Figure 10 is a plot of the resulting RMS errors in each fit as function of the delay used in the daily index. This figure shows that the smallest RMS error was obtained for a delay of 3 days in the Ca index for the maximum temperatures. This delay, however, is rather uncertain since it changed as the form of the equation changed. A three day
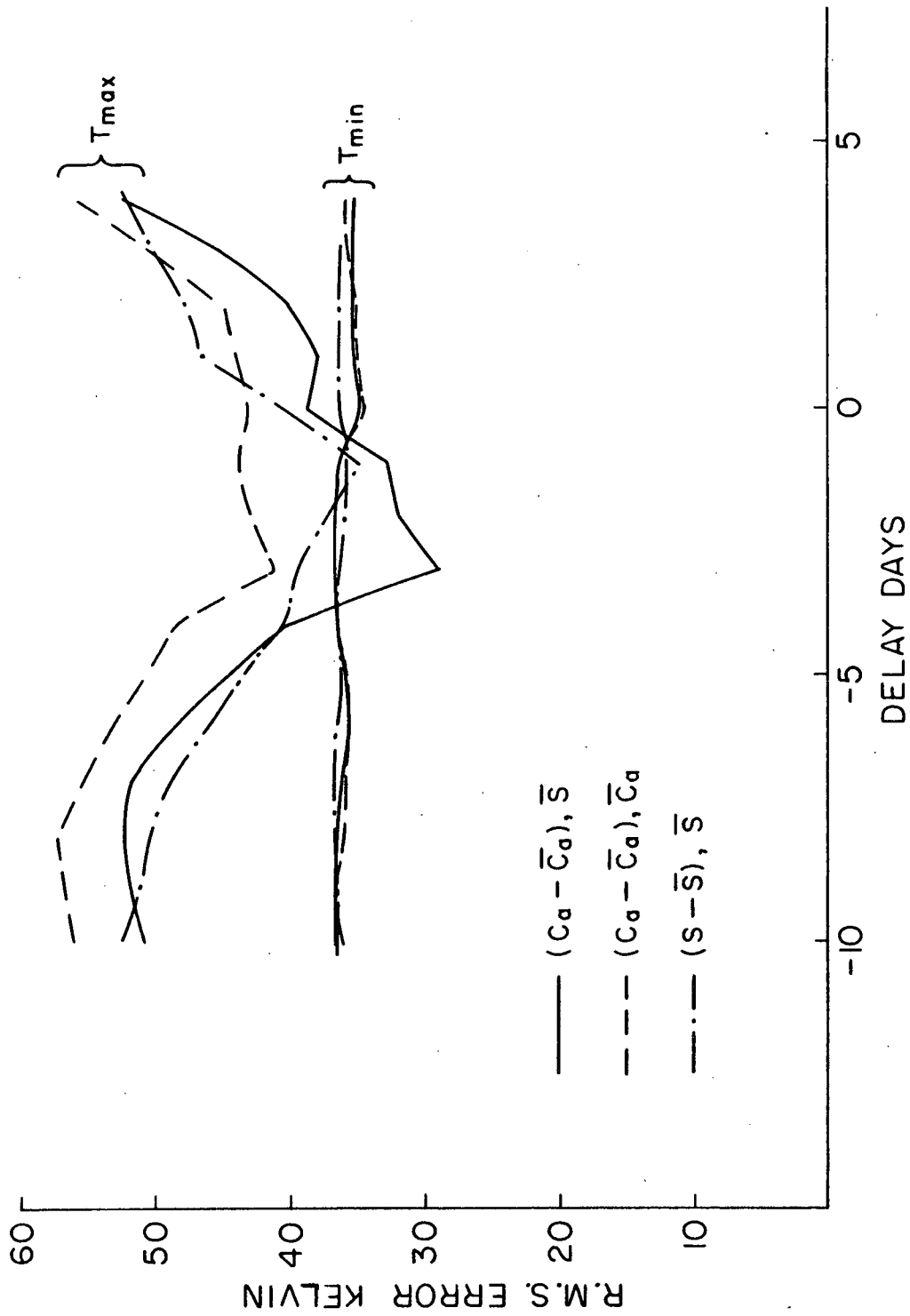
FIGURE 10: RMS Errors in Fits of Incoherent Scatter Temperatures as a
Function of Delay used for Index.

delay is rather hard to explain physically and is possibly
just a result of the small amount of data used for the
maximum temperatures.

Table 1 indicates that the optimum fit for the maxi-
mum temperatures was obtained for a combination of $(Ca - \overline{Ca})$
and $S_{10.7}$. The $(Ca - \overline{Ca})$ term is intended to model the
effect on the upper atmosphere caused by short term
(27 day) variations in the active regions of the sun,
while the $\overline{S}_{10.7}$ term models the effect of the long term
variations in the sun's radiation. The result of fitting
the temperature minimum from Arecibo incoherent scatter
data and for the ionosonde data are shown in Table 2.
Again the smallest deviations were obtained using the
average monthly 2800 MHz flux and the $(Ca - \overline{Ca})$ to model the
short term variations.

The terms in the equations for the two fits are
different and it is of importance to reconcile the differ-
ences and decide to what extent each can be used to provide
valid information about the thermospheric temperature.
While it has been shown that a uniformly decaying ionosphere
will tend to a Chapman C_α layer the conditions at Arecibo
are considerably different from this simple model and the
effect of neutral winds, for example, have a profound
effect on the layer behavior during the night. While it
might be argued that the layer shape parameters should be
linearly related to temperature the actual assumption of

$$SCAT = .815 H$$

TABLE 1: Maximum Temperature

$$T_{MAX} = G_1 + G_2 X + G_3 K_p + G_5 \sin \frac{4\pi}{365} (D + G_4) + G_6 Y$$

X	Y	G_1 Coef.	Std. Error	G_2 Coef.	Std. Error	G_3 Coef.	Std. Error	RMS Error in Fit
Ca - $\overline{Ca}$	$\overline{Ca}$	1005	68.4	3.69	1.02	20.4	11.3	41.3
S - S	$\overline{S}$	425	141	2.65	0.629	9.08	9.45	35.1
Ca - $\overline{Ca}$	$\overline{S}$	657	102	4.08	0.729	17.6	7.64	29.3

X	Y	G_4 Coef.	Std. Error	G_5 Coef.	Std. Error	G_6 Coef.	Std. Error	RMS Error in Fit
Ca - $\overline{Ca}$	Ca	127	57	11.1	19.1	3.51	1.55	41.3
S - $\overline{S}$	$\overline{S}$	167	8	66.1	15.5	5.37	1.04	35.1
Ca - $\overline{Ca}$	$\overline{S}$	132	14	30.9	13.9	3.63	0.742	29.3

Note: In fitting these data the following were used. Ca for D - 3 corrected for solar distance, K_p for H - 6 where D is the day number and H is the UT in hours.

TABLE 2: Minimum Temperature

$$T_{MIN} = G_1 + G_2 X + G_3 K_p + G_5 \sin \frac{4\pi}{365} (D + G_4) + G_6 Y$$

	X	Y	G$_1$ Coef.	G$_1$ Std. Error	G$_2$ Coef.	G$_2$ Std. Error	G$_3$ Coef.	G$_3$ Std. Error
Incoherent Scatter	Ca – $\overline{Ca}$	$\overline{Ca}$	752	60.5	1.08	0.779	16.4	8.40
	S – S	S	703	139	0.362	0.665	15.9	8.97
	Ca – $\overline{Ca}$	S	701	121	0.931	0.764	17.6	8.48
Ionogram SCAT	Ca – $\overline{Ca}$	$\overline{Ca}$	616	19.5	1.19	0.499	30.21	4.57
	S – S	S	451	28.5	0.714	0.338	27.69	4.45
	Ca – $\overline{Ca}$	S	451	28.5	1.085	0.485	28.15	4.45

TABLE 2: Continued

	X	Y	G₄ Coef.	G₄ Std. Error	G₅ Coef.	G₅ Std. Error	G₆ Coef.	G₆ Std. Error
Incoherent Scatter	Ca – $\overline{Ca}$	$\overline{Ca}$	146	19	22.7	16.1	1.50	1.21
	S – $\overline{S}$	$\overline{S}$	143	13	34.3	16.3	0.852	0.973
	Ca – $\overline{Ca}$	$\overline{S}$	144	14	30.2	15.9	0.838	0.822
Ionogram SCAT	Ca – $\overline{Ca}$	$\overline{Ca}$	72	16	18.39	9.78	4.04	0.42
	S – $\overline{S}$	S	83	16	18.06	9.57	2.54	0.21
	Ca – $\overline{Ca}$	$\overline{S}$	82	15	18.71	9.55	2.53	0.21

Note: In fitting these data the following were used. Ca and $S_{10.7}$ for D and K_p for H – 6.

may be in error. If we assume $K_p = 0$, $Ca - \overline{Ca} = 0$ we can calculate the neutral temperatures for a value of S of 140 for both sets of data. This gives 805 K for the SCAT data as opposed to 818 K for the incoherent scatter results. It thus appears that the relation between the layer half thickness and the temperature is reasonably consistent with the two sets of data. It is known that at Puerto Rico the layer drops after midnight as has been discussed by Nelson and Cogger (1971). Such drops have been observed to result in changes in the shape of the F layer. Nisbet and Quinn (1963) investigated the effect of the vertical velocity of $h_m F_2$ on the ratio of SCAT values for Puerto Rico to temperatures calculated from the solar flux. This investigation showed no effect on this relationship as the rates of change of the height of the F layer maximum changes by $\pm$ 50 km./hour. The rms errors for the temperatures for individual days were 5.6 times larger for the temperatures from the SCAT values; however, the much larger number of points and the greater range of solar activities resulted in statistically better fits. Caution should, however, be observed as such large statistical fluctuation may not be random but could possibly result from some undetermined non-linear errors associated with the ionogram reduction procedure.

The terms related to the quiet monthly average temperatures G_1 and G_6 are rather different for the incoherent scatter and ionosonde data. The main difference is that the

constant term is much smaller for the ionosonde data and the term multiplying the monthly mean solar index is larger. It is believed that this is a real effect and is probably due to the much larger range of solar activities for the ionosonde data. It is possible that the effect results from an increased dependence of the temperature on solar activity under active, compared with quiet solar conditions. Over the range of solar activities present in the incoherent scatter data the range of temperatures calculated by the two formula are

2800 MHz Flux $\overline{S}$	120	167
Incoherent scatter	T = 801	T = 838
Ionosonde data	T = 755	T = 874

These differences are not large compared with the standard deviations in either set of data. It is believed that the terms derived from the ionosonde data probably provide a better fit over wide ranges of solar activity.

The terms related to the differences between the daily and monthly average solar indices agree within the standard errors for both sets of data. It is important to note that the term itself is very small and for a typical solar rotation period would only amount to between 7 and 14 K.

The term dependent on the K_p value is considerably larger for the ionosonde fits than for the incoherent scatter data. This is probably a real effect. The range of magnetic activities for the ionosonde data was 0 to 8.6

and for the incoherent scatter data was from 0 to 4.
Orbital decay measurements indicate a non-linear variation
in the K_p term.

The amplitudes of the semi-annual term are within the
error limits for the two sets of data. The phase terms
indicate a two month difference in phase. This is rather
large for a semi-annual term and could well result from
a phase change related to the level of solar activity.
It is also possible that the difference results from the
correlation of some other parameter such as the K_p index
with the semi-annual period.

3.2 An Empirical Function for the Exospheric Temperature

The following Fourier series was derived to describe
the exospheric temperatures at a given latitude.

$$T_\infty(t) = T_{min} + (T_{max} - T_{min})$$

$$\cdot \left\{ A_o + \sum_{y=1}^{5} \left[A_j \cos(\frac{2\pi j}{24} t) + Bj \, Sin(\frac{2\pi j}{24} t) \right] \right\} \quad (15)$$

where

$$T_{min} = \text{diurnal minimum (K)}$$

$$T_{max} = \text{diurnal maximum (K)}$$

$$A_D = 1.809 + (0.007286D - 0.1998)D$$

$$A_j = \frac{X_j + R_y \cos aj}{b}$$

$$B_y = \frac{Y_y + R_y \sin aj}{b}$$

$$A_y = 0.01745 \left[C_{1y} + (C_{2y} + C_{3y}D)D \right]$$

$$b = 0.4661 + \left[0.06758 - 0.002093\ D \right] D$$

$$t = \text{time in hours counting from midnight}$$

and where D is daylength at 200 km given by

$$D = \frac{24}{\pi} \cos^{-1} \left\{ \frac{-0.1738 - \sin Lg \sin}{\cos Lg \ \cos \delta} \right\}$$

$$Lg = \text{geographic latitude in radians}$$

$$\delta = \text{solar declination in radians approximated}$$
by

$$\delta = 0.40915 \cos \left[\frac{2\pi}{365.25} (N + 8) \right]$$

$$N = \text{day number of the year counting from}$$
January 1

The required coefficients are given in Table 3.

The functions used for the diurnal maximum and minimum temperatures in equation (15) are given by:

$$T_{max} = T_3 + T_2 + T_1 \cos \left| Lg - \delta \right| \qquad (16)$$

$$T_{min} = T_3 + T_2 - T_1 \cos \left| Lg + \delta \right| \qquad (17)$$

where

$$T_1 = 16.2 + 1.19\ S_{10.7}$$

TABLE 3: Coefficients for Exospheric Temperature

j	X_j	Y_j	C_{1j}	C_{2j}	C_{3j}	B_j
1	0.0	0.0	- 75.55	- 4.7698	0.07937	0.45
2	0.05	-0.08	323.51	-42.606	1.9511	0.14
3	0.016	0.034	311.05	8.873	-1.8354	0.031
4	0.025	0.002	114.20	-74.034	4.3320	0.03
5	-0.01	-0.015	391.81	-82.156	4.5966	0.0131

$$T_2 = [16.0 \, K_p + 0.05 \, \exp \, (K_p)][1.0 + 0.72 \, \cos \, (2L_m - \pi)]$$

$$T_3 = [0.338 \, (S_{10.7} - \overline{S}_{10.7}) - 0.159 S_{10.7} - 2.65] \sin \left\{ \frac{4\pi N}{365.25} \right\} + 1.5$$

$$+ 535.0 + 2.98 S_{10.7} - 1.48 \, (S_{10.7} - \overline{S}_{10.7})$$

$S_{10.7}$ = daily 2800 MHz index

$\overline{S}_{10.7}$ = average 2800 MHz index for previous solar rotation

L_m = geomagnetic latitude in radians

The variations due to geomagentic activity given by T_2 is based on data from Arecibo, the results of Waldteufel (1970), Blamont and Luton (1970), and assumes the effect to be inversely proportional to the distance to the auroral zone. This dependence, shown in Figure 11, is meant to give only the general behavior for moderate geomagnetic activity and cannot be expected to reproduce the temperatures following a given magnetic storm. It should also be noted that the dependence on solar activity given by T_3 and T_1 is based only on the 2800 MHz index even though it was reported in section 3.1 that a combination including the Ca II index gave better correlation with the neutral temperatures. This was done to keep the temperature model on the same basis as the Jacchia density model used.

The 300 km. atomic oxygen densities of the Jacchia (1970 b) model were fitted to the following function of T_j:
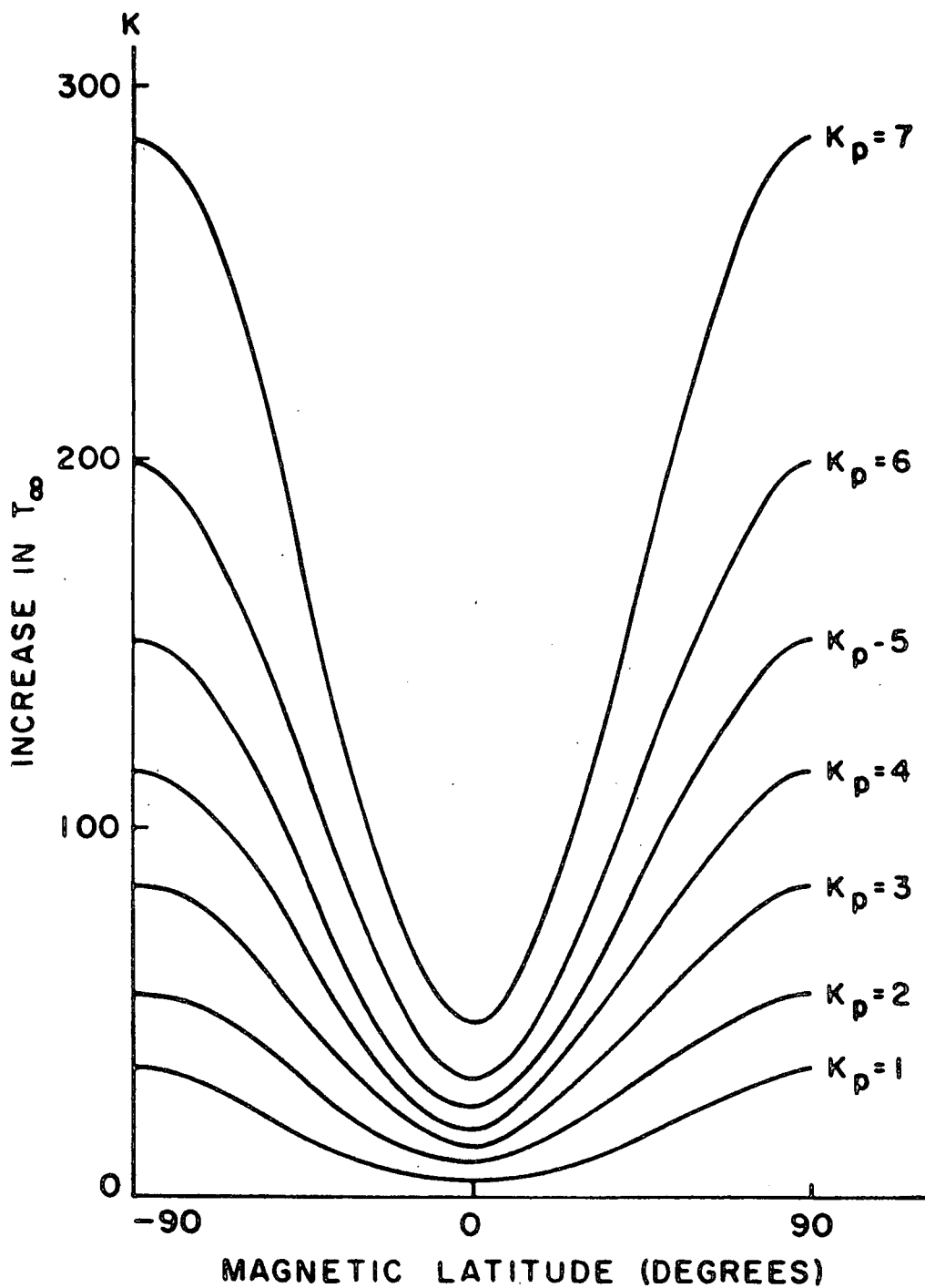
FIGURE 11:   Increase in T_∞ with K_p Daytime Maximum.

$$n(0, 300) = 10^{\sum_{i=0}^{4} m_i T_j^i} \tag{18}$$

where

$$M_0 = 8.177$$

$$M_1 = 0.2919$$

$$M_2 = -3.483 \times 10^{-6}$$

$$M_3 = 2.238 \times 10^{-9}$$

$$M_4 = -5.643 \times 10^{-13}$$

and T_j is calculated by the formulas given by Jacchia (1970 b).

3.3 An Empirical Relationship for the Temperature Gradient at 120 Km.

After the temperature gradients were calculated by the iterative process described in section 2.5, each data set was Fourier analyzed. The resulting Fourier coefficients were then averaged according to season. Table 4 lists the Fourier coefficients for each season and should be used in the following equation.

$$\frac{dT}{dz}\bigg|_{Z = 120} = \sum_{j=0}^{6} A_j \cos \frac{2\pi j}{24} t + B_j \sin \frac{2\pi j}{24} t$$

TABLE 4: Fourier Coefficients for the Temperature Gradient at 120 Km.

Spring & Fall

K	A_K	B_K
0	8.483	0.0
1	-1.102	-0.908
2	0.0949	0.205
3	-0.157	-0.00977
4	-0.10	0.00633
5	-0.00458	0.0051
6	0.123	0.0448

Winter

K	A_K	B_K
0	7.550	0.0
1	-1.323	-0.928
2	0.0126	0.330
3	-0.0593	-0.105
4	0.111	-0.106
5	0.0634	-0.541
6	-0.0955	-0.0434

TABLE 4:   Continued

Summer

K	A_K	B_K
0	7.15	0.0
1	-1.135	-1.147
2	0.104	0.299
3	-0.120	-0.0729
4	-0.126	-0.0465
5	0.0205	-0.0765
6	-0.00713	0.00464

CHAPTER 4

CONCLUSIONS

4.1 Compatibility of Satellite Orbital Decay Data with Incoherent Scatter Temperatures

It has been shown that satellite orbital decay densities can be made compatible with temperatures deduced from incoherent scatter measurements. This has been done by allowing the temperature gradients at 120 km. to vary.

In a Fourier analysis of the temperature gradients it was found that the ratio of the semi-diurnal to diurnal component varied from 0.16 at equinox to 0.20 in the winter. This seems to contradict the hypothesis of constant boundary conditions at 90 km. If these tides were present they should be reflected in the temperature gradients which would increase the semi-diurnal component substantially. This was not seen in this study. However, it is cautioned that the choice of constant boundary conditions at 120 km. which were used to calculate the temperature gradients probably affected the results.

4.2 Seasonal Variations in the Diurnal Profile of the Exosphere Temperature

The Arecibo data presented in this analysis has shown that the time of the temperature maximum has varied from the 1500 hours in the winter to 1600 hours in the spring and fall, and finally to 1700 hours in the summer. The time of the minimum varied from 500 hours in the winter to 400 hours in the spring and fall, and to about 300 hours

in the summer. This clearly reflects the change in day-
length at Arecibo and it was therefore concluded that a
daylength parameter should be used to model the seasonal
variations in the diurnal profile of the exospheric tempera-
ture. Recently, Salah and Evans (1972) have shown that
the same type of variation can be seen at Millstone Hill
which further supports the use of a daylength parameter.

In a Fourier analysis of the exospheric temperatures
it was found that both the diurnal and semi-diurnal compo-
nents exhibit a seasonal variation. For a daylength of
18 hours (summer) it was found that the semi-diurnal
component was only about 25% of the diurnal component.
For a daylength of 9 hours (winter), the semi-diurnal
component was almost 45% that of the diurnal component.
This seems to agree with Salah and Evans (1972) who give
a figure of 30% for a spring day which should fall between
the two values given here. The phasing of both components
also varied seasonally.

4.3 Usefulness of the Calcium Plage and Monthly Mean 2800 MHz Indices in an Empirical Model

For the daytime maximum values the formula incorpo-
rating the mean monthly 2800 MHz index and the difference
between the daily and monthly mean Ca II indices was better
at the 80% confidence level than that based on the 2800 MHz
indices alone and at the 94% level than that based on the
Ca II index alone. The differences between the different
indices for the nighttime temperatures are not believed

to be significant. To this extent our measurements confirm the observation of Prag and Morse (1970) that the variations in EUV over a solar rotation are better correlated with the Ca II index than with 2800 MHz solar flux. This was not true for the long term fluctuations.

Our observations show that the nighttime minimum temperature is less sensitive by a factor of about four to the day to day fluctuations in the solar activity than is the diurnal maximum. This means that the day to night temperature ratio is larger for days on which the sun is active than for days on which it is quiet. This behavior is very different from that given in models such as CIRA (1965) or Jacchia (1970, 1971). A similar but smaller difference exists in the terms dependent on the mean monthly solar activity and our observations would indicate that the monthly average day to night temperature ratio would increase from 1.3 to 1.55 from low to high solar activity.

The present measurements indicate a semi-annual term at Arecibo of about 30 K. This term is rather difficult to determine from the limited amount of incoherent scatter data, and further measurements will be required before unambiguous results can be obtained. It does not look, however, as if the effect is confined to the boundary densities alone as has been suggested by Jacchia (1971 b).

It would appear that though a combination of the Ca II and 2800 MHz indices is better able to serve as an index of the solar flux controlling the thermospheric temperatures,

any such improvement is small. It is to be hoped that in the near future satellite monitoring will enable a solar index to be developed based on an integral of the solar EUV flux suitably weighted by the cross section of the atmospheric constituents.

BIBLIOGRAPHY

Banks, P., Collision frequencies and energy transfer: electrons, Planetary Space Sci., 14, 1085-1103, 1966.

Banks, P., Collision frequencies and energy transfer: ions, Planetary Space Sci., 14, 1105-1122, 1966.

Bates, D. R., Some problems concerning the terrestrial atmosphere above about the 100 km. level, Proc. Roy. Soc., A253, 451-462, 1959.

Bauer, P., P. Waldteufel, and D. Alcayde, Diurnal Variations of the Atomic Oxygen Density and Temperature from Incoherent Scatter Measurements in the Ionospheric F Region, J. Geophysical Res., 75(25), 4825-4832, 1970.

Carru, H., M. Petit, and P. Waldteufel, On the diurnal variation of the thermopause temperature, Planetary Space Sci., 15, 944-945, 1967.

Carru H., M. Petit, G. Vasseur, P. Waldteufel, Resultats ionospheriques obtenus par diffusion de Thompson, Annales de Geophysique, 23(4), 455-465, 1967.

Carru, H., and P. Waldteufel, Étude par diffusion de Thompson des variations de la temperature exospherique, Annales de Geophysique, 25(2), 485-494, 1969.

Chandra, S., and P. Stubbe, The diurnal phase anomaly in the upper atmospheric density and temperature, Planetary Space Sci., 18, 1021-1033, 1970.

CIRA, COSPAR International Reference Atmosphere, North-Holland, Publishing Co., Amsterdam, 313 pp. 1965.

Freidman, M.P., A three-dimensional model of the upper atmosphere, Smithsonian Astrophys. Obs., Spec. Rpt. No. 250, 1-101, September 19, 1967.

Freidman, M.P., Upper atmosphere dynamics, Smithsonian Astrophys. Obs., Spec. Rpt. No. 316, 1-52, May 28, 1970.

Hall, L. A., J. E. Higgins, C. W. Chagnon, and H. E. Hinteregger, Solar-cycle variation of extreme ultra-violet radiation, J. Geophysical Res., 74, 4181, 1969.

Harris, I. and W. Priester, Time-dependent structure of the upper atmosphere, NASA Technical Note D-1443, 1-71, July 1962.

Harris, I., and W. Priester, Theoretical models for the solar-cycle variation of the upper atmosphere, J. Geophysical Res., 67(12), 4585-4591, November 1962.

Jacchia, L. G., A variable atmospheric-density model from satellite accelerations, Smithsonian Astrophys. Obs., Spec. Rpt. No. 39, March 30, 1960.

Jacchia, L. G., A working model for the upper atmosphere, Nature, 192, 1147-1148, December 23, 1961.

Jacchia, L. G., Static diffusion models of the atmosphere with empirical temperature profiles, Smithsonian Contr. Astrophys., 8, 215-257, 1965; also in Smithsonian Astrophys. Obs. Spec. Rpt. No. 170, December 1964.

Jacchia, L. G., Density variations in the heterosphere, Annales de Geophysique, 22(1), 75-85, 1966.

Jacchia, L. G., Recent results in the atmospheric region above 200 km. and comparisons with CIRA 1965, Space Res. VIII, ed. by A. P. Mitra, L. G. Jacchia, and W. S. Newman (North-Holland Pub. Co., Amsterdam), 800-810, 1968; also in Smithsonian Astrophys. Obs. Spec. Rpt. No. 245, 25 pp., 1967.

Jacchia, L. G., New static models of the thermosphere and exosphere with empirical temperature profiles, Smithsonian Astrophys. Obs. Spec. Rpt. No. 313, 1-88, May 6, 1970a.

Jacchia, L. G., Private communication, July 16, 1970.

Jacchia, L. G., Revised static models of the thermosphere and exosphere with empirical temperature profiles, Smithsonian Astrophys. Obs. Spec. Rpt. 332, 113, 1971.

Jacchia, L. G., Semiannual variation in the Heterosphere: A reappraisal, J. Geophysical Res., 76(19), 4602-4607, July 1, 1971.

Johnson, F. S., Temperature Distribution of the Ionosphere under Control of Thermal Conductivity, J. Geophysical Res., 61(1), 71-76, March, 1956.

King-Hele, D. G., Decrease in upper-atmosphere density since the sunspot maximum of 1957-58, Nature, 198, 832-834, 1963.

King-Hele, D. G. and J. Hingston, Variation in air density at heights near 150 km. from the orbit of the satellite 1966-101J, Planetary Space Sci., 15, 1883-1893, 1967.

King-Hele, D. G. and J. Hingston, Air density at heights near 190 km. from the orbit of SECOR 6, Planetary Space Sci., 16, 675-691, 1968.

Kohl, H., and J. W. King, Atmospheric winds between 100 and 700 km. and their effects on the ionosphere, Fifteenth URSI General Assembly, Munich, September 1966.

Marov, M. Y., Density of the upper atmosphere from data of Soviet satellite drag, Space Res. V, (North-Holland Pub. Co., Amsterdam), 1140-1149, 1965.

Marov, M. Y., Soviet data on densities and scale heights at altitudes greater than 150 km., Space Res. VIII, (North-Holland Pub. Co., Amsterdam), 811-820, 1968.

May, B. R., A note on the feature and cause of the diurnal variation of neutral air density at 205 km., Planetary Space Sci., 11, 1273-1275, 1963.

McClure, J. P., Diurnal variation of neutral and charged particle temperature in the equatorial F-region, J. Geophysical Res., 74(1), 279-291, 1969.

Minzner, R. A., and W. S. Ripley, The ARDC model atmosphere 1956, Air Force Surveys in Geophysics No. 86, Geophysics Research Directorate, Air Force Cambridge Research Center, December 1956.

Minzner, R. A., K. S. W. Champion, and H. L. Pond, The ARDC model atmosphere 1959, Air Force Surveys in Geophysics No. 115, Geophysics Research Directorate, Air Force Cambridge Research Center, August 1959.

Nelson, G. J. and L. L. Cogger, Enhancements in electron content at Arecibo during geomagnetic storms, Planetary Space Sci., 19, 761-775, 1971.

Nicolet, M., and P. Mange, An Introduction to the Study of the Physical Constitution and Chemical Composition of the High Atmosphere, Ionosphere Research Scientific Report No. 35, The Pennsylvania State University, April 15, 1952.

Nicolet, M., The constitution and composition of the upper atmosphere, Proc. IRE, 47(2), 142-147, February 1959.

Nicolet, M., The properties and constitution of the upper atmosphere, Physics of the Upper Atmosphere, ed. by J. A. Ratcliffe (Academic Press, New York), 17-71, 1960.

Nicolet, M., Structure of the Thermosphere, Ionosphere
    Research Scientific Report No. 134, The Pennsylvania
    State University, July 1, 1960.

Nicolet, M., Les variations de la densité et du transport
    de chaleur par conduction dans l'atmosphère supérieure,
    Space Res. I, ed. by H. Kallmann-Bijl (North Holland
    Pub. Co., Amsterdam), 46-89, 1960.

Nicolet, M., Density of the heterosphere related to tempera-
    ture, Smithsonian Contr. Astrophys., 6, 175-187, 1963;
    also in Smithsonian Astrophys. Obs. Spec. Rpt. No.
    75, 1-30, 1961.

Nicolet, M., A representation of the terrestrial atmosphere
    from 100 km. to 3000 km., Ionosphere Research Scientific
    Report No. 155, The Pennsylvania State University,
    February 1, 1962.

Nicolet, M., Solar radioflux and upper-atmosphere tempera-
    ture, Ionosphere Research Scientific Report No. 195,
    The Pennsylvania State University, October 1, 1963.

Nisbet, J. S., Neutral atmospheric temperature from
    incoherent scatter observations, J. Atmospheric
    Sciences, 24(5), 586-593, 1967.

Nisbet, J. S. and T. P. Quinn, The recombination coefficient
    of the nighttime F layer, J. Geophysical Res., 68(4),
    1031-1038, 1963.

Prag, A. B. and F. A. Morse, Variations in the solar ultra-
    violet flux from July 13 to August 9, 1968, J. Geophys-
    ical Res., 75(25), 4613-4621, 1970.

Priester, A., H. A. Martin, and K. Kramp, Diurnal and
    seasonal density variations in the upper atmosphere,
    Nature (London), 188, 202-204, 1960.

Quinn, T. P. and J. S. Nisbet, Recombination and transport
    in the nighttime F layer of the ionosphere, J. Geophys-
    ical Res., 70(1), 113-130, January 1, 1965.

Rocket Panel, The, Pressures, densities, and temperatures in
    the upper atmosphere, The Physical Review, 88, No. 5,
    1027-1032, 1952.

Stein, J. A. and J. C. G. Walker, Models of the upper
    atmosphere for a wide range of boundary conditions,
    J. Atmospheric Sciences, 22, 11-17, 1965.

Stubbe, P., Simultaneous solution of the time dependent coupled continuity equations, heat conduction equations, and equations of motion for a system consisting of a neutral gas, an electron gas, and a four component ion gas, J. Atmospheric Terrestrial Phys., 32, 865-903, 1970.

Stubbe, P., Vertical neutral gas motions and deviations from the barometric law in the lower thermosphere, Planetary Space Sci., 20, 209-215, 1972.

Swartz, W. E. and J. S. Nisbet, Diurnal variation of the neutral temperature profile at Arecibo from incoherent scatter measurements and its relevance to the 1400 hour density maximum, J. Geophysical Res., 76(1), 185-196, January 1, 1971; also in The Pennsylvania State University Ionosphere Research Scientific Report No. 364, October 15, 1970.

Taeusch, D. R., H. B. Niemann, G. R. Carignan, R. E. Smith, and J. O. Ballance, Diurnal survey of the thermosphere (1) neutral particle results, Space Res. VIII, ed. by A. P. Mitra, L. G. Jacchia, and W. S. Newmann (North-Holland Pub. Co., Amsterdam), 930-939, 1968.

Timothy, A. F. and J. G. Timothy, Long-term intensity variations in the solar helium II Lyman Alpha line, J. Geophysical Res. 75(1), 4613-4621, September 1, 1970.

Volland, H., On the dynamics of the upper atmosphere, Space Res. VII, ed. by R. L. Smith-Rose (North-Holland Pub. Co., Amsterdam), 1193-1203, 1967.

Volland, H., A theory of thermospheric dynamics - I: Diurnal and solar cycle variation, Planetary Space Sci., 17, 1581-1597, 1969.

Waldteufel, P., Un étude par diffusion incohérente de la haute atmosphère neutre, Ph.D. thesis, Faculté des Sciences de Paris, 1970.

Woodgate, B. E., D. E. Knight, R. Uribe, P. Sheather, J. Bowles, and R. Nettleship, Extreme ultraviolet line intensities from the sun, accepted for publication in the Proceedings of the Royal Society of London, 1972.